

Supporting information

Influence of alkyl chain length on the photovoltaic properties of dithienopyran-based hole-transporting materials for perovskite solar cells

Mauricio Caicedo-Reina,^{‡a} Manuel Pérez-Escribano,^{‡b} Javier Urieta-Mora,^{c,d} Inés García-Benito,^{c,d} Joaquín Calbo,^b Enrique Ortí,^{*b} Agustín Molina-Ontoria,^{*d} Alejandro Ortiz,^{a,e} Braulio Insuasty^{*a,e} and Nazario Martín^{*c,d}

^a *Grupo de Investigación de Compuestos Heterocíclicos, Departamento de Química, Facultad de Ciencias Naturales y Exactas, Universidad del Valle, Calle 13 #100-00, 25360, Cali, Colombia. E-mail: braulio.insuasty@correounivalle.edu.co*

^b *Instituto de Ciencia Molecular, Universidad de Valencia, Catedrático José Beltrán 2, 46980 Paterna, Spain. E-mail: enrique.orti@uv.es*

^c *IMDEA-Nanociencia, C/ Faraday 9, Ciudad Universitaria de Cantoblanco, 28049, Madrid, Spain.*

^d *Departamento de Química Orgánica, Facultad C. C. Químicas, Universidad Complutense de Madrid, Av. Complutense s/n, 28040, Madrid, Spain. Homepage: <http://ucm.es/info/fullerene/>. E-mail: nazmar@ucm.es, amolinao@ucm.es*

^e *Center for Research and Innovation in Bioinformatics and Photonics-CIBioFi, Calle 13 #100-00, Edificio E-20, No. 1069, 25360, Cali, Colombia.*

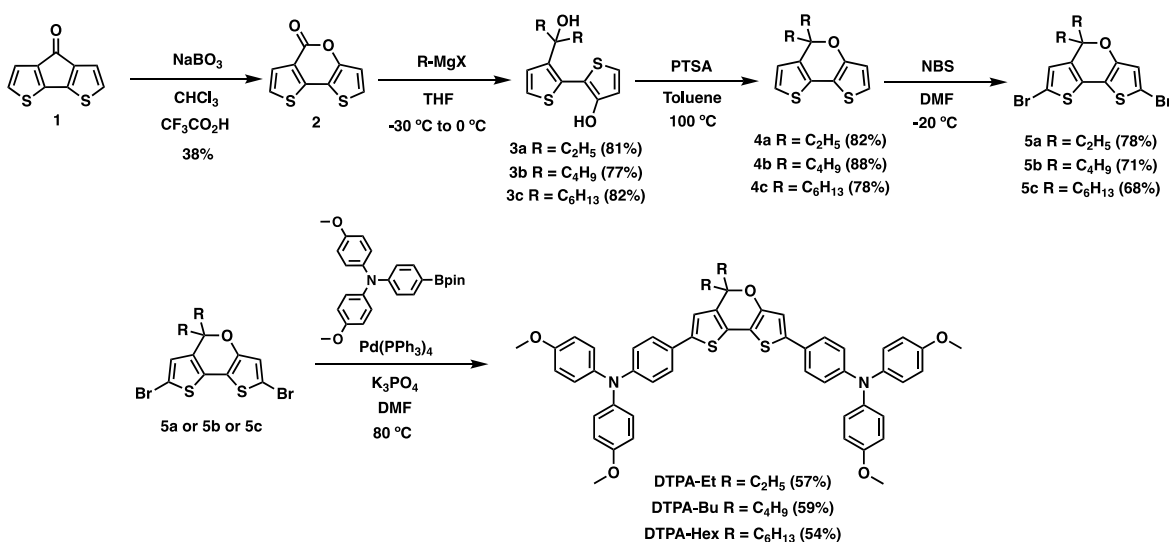
[‡] *These authors have contributed equally to the work.*

1. Experimental section.

General methods: Chemicals and reagents were purchased from commercial suppliers and used as received. All solvents were dried according to standard procedures. Air-sensitive reactions were carried out under argon atmosphere. The device preparation was done in a glovebox under nitrogen atmosphere. Flash chromatography was performed using silica gel (Merck, Kieselgel 60, 230–240 mesh or Scharlau 60, 230–240 mesh). Analytical thin-layer chromatography (TLC) was performed using aluminum-coated Merck Kieselgel 60 F254 plates. NMR spectra were recorded on a Bruker Advance 300 (^1H : 400 MHz; ^{13}C : 101 MHz) spectrometer at 298 K using partially deuterated solvents as internal standards. Coupling constants (J) are denoted in Hz and chemical shifts (δ) in ppm. Multiplicities are denoted as follows: s = singlet, d = doublet, t = triplet, m = multiplet. FT-IR spectra were recorded on a Bruker Tensor 27 (ATR device) spectrometer. UV-Vis spectra were recorded in a Varian Cary 50 spectrophotometer. Matrix-assisted laser desorption ionization coupled to a time-of-flight analyzer (MALDI-TOF) mass spectrometry experiments were recorded on a MAT 95 thermo spectrometer and a Bruker REFLEX spectrometer. Cyclic voltammetry (CV) experiments were conducted in 0.1 M solution of NBu_4PF_6 in CH_2Cl_2 . Glassy carbon electrode was used as a working electrode and platinum wires were used as counter and reference electrodes. Before each measurement, solutions were deoxygenated with N_2 . Ferrocene was added as an internal standard; its oxidation potential in CH_2Cl_2 was positioned at 0.8 V vs. normal hydrogen electrode (NHE) and HTMs oxidation potentials were recalculated in reference to NHE. Thermogravimetric analysis (TGA) was performed using a TA Instruments TGAQ500 with a ramp of 10 $^\circ\text{C}/\text{min}$ under N_2 from 100 to 1000 $^\circ\text{C}$. Differential scanning calorimetry (DSC) was run on a Discovery DSC from TA instruments. Three cycles were recorded under nitrogen, heating (until 400 $^\circ\text{C}$) and cooling (50 $^\circ\text{C}$) at 20 $^\circ\text{C}/\text{min}$ of scanning rate.

2. Synthetic details and characterization.

Compounds **1**^[1], **2**^[2], **3**^[3] and **4**^[3] were prepared according to previously reported synthetic procedures and showed identical spectroscopic properties to those reported therein.



Scheme S1. Synthetic methodology for the preparation of **DTPA-Et**, **DTPA-Bu** and **DTPA-Hex**.

Compound 3a. A solution of compound **2** (200 mg, 0.96 mmol) in dry THF (10 mL) was cooled to $-30\text{ }^{\circ}\text{C}$ and degassed for 20 minutes. After that, 0.93 mL (2.88 mmol) of a 3.0 M ethylmagnesium bromide solution in diethyl ether was added dropwise. Then, the solution was stirred for 1 hour at $-30\text{ }^{\circ}\text{C}$ and 1.5 hours at $0\text{ }^{\circ}\text{C}$. Water was added and the product was extracted in ethyl acetate.

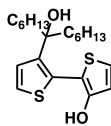
The organic phase was dried over anhydrous sodium sulfate. The solvent was removed under reduced pressure and the crude product was purified by column chromatography on silica gel (dichloromethane/hexane, 7:1) to afford a pale yellow oil (194 mg, yield: 81%). ¹H NMR (400 MHz, CDCl₃) δ /ppm 7.99 (s, 1H), 7.29 (d, $J = 8.0$ Hz, 1H), 7.17 (d, $J = 4.0$ Hz, 1H), 6.94 (d, $J = 8.0$ Hz, 1H), 6.74 (d, $J = 4.0$ Hz, 1H), 2.34 (s, 1H), 1.95–1.86 (m, 4H), 0.84 (t, $J = 8.0$ Hz, 6H); ¹³C NMR (100 MHz, CDCl₃) δ /ppm 151.5, 133.3, 129.4, 124.8, 120.8, 120.7, 118.7, 110.3, 87.2, 32.4, 8.4.

Compound 3b. A solution of compound **2** (150 mg, 0.72 mmol) in dry THF (10 mL) was cooled to $-30\text{ }^{\circ}\text{C}$ and degassed for 20 minutes. After that, 1.10 mL (2.16 mmol) of a 2.0 M butylmagnesium chloride solution in THF was added dropwise. Then, the solution was stirred for 1 hour at $-30\text{ }^{\circ}\text{C}$ and 1.5 hours at $0\text{ }^{\circ}\text{C}$. Water was added and the product was extracted in ethyl acetate. The

organic phase was dried over anhydrous sodium sulfate. The solvent was removed under reduced pressure and the crude product was purified by column chromatography on silica gel (dichloromethane/hexane, 4:1) to afford a pale green oil (180 mg, yield: 77%). ¹H NMR (400 MHz, CDCl₃) δ /ppm 8.05 (s, 1H), 7.26 (d, J

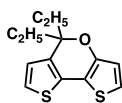
= 8.0 Hz, 1H), 7.17 (d, $J = 4.0$ Hz, 1H), 6.94 (d, $J = 8.0$ Hz, 1H), 6.72 (d, $J = 4.0$ Hz, 1H), 2.46 (s, 1H), 1.91–1.78 (m, 4H), 1.29–1.15 (m, 8H), 0.85 (t, $J = 8.0$ Hz, 6H); ^{13}C NMR (100 MHz, CDCl_3) δ /ppm 151.3, 132.9, 129.0, 124.8, 120.8, 120.7, 118.7, 110.3, 86.6, 39.9, 26.1, 23.2, 14.2.

Compound 3c. A solution of compound **2** (150 mg, 0.72 mmol) in dry THF (10 mL) was cooled to -30°C and degassed for 20 minutes. After that, 1.1 mL (2.16 mmol) of a 2.0 M hexylmagnesium bromide solution in THF was added dropwise. Then, the solution was stirred for 1 hour at -30°C and 1.5 hours at 0°C . Water was added and the product was extracted in ethyl acetate. The



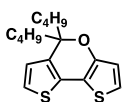
organic phase was dried over anhydrous sodium sulfate. The solvent was removed under reduced pressure and the crude product was purified by column chromatography on silica gel (dichloromethane/hexane, 4:1) to afford a pale green oil (192 mg, yield: 88%). ^1H NMR (400 MHz, CDCl_3) δ /ppm 8.03 (s, 1H), 7.25 (d, $J = 4.0$ Hz, 1H), 7.16 (d, $J = 4.0$ Hz, 1H), 6.91 (d, $J = 4.0$ Hz, 1H), 6.71 (d, $J = 4.0$ Hz, 1H), 2.43 (s, 1H), 1.89–1.82 (m, 4H), 1.25–1.20 (m, 16H), 0.83 (t, $J = 8.0$ Hz, 6H); ^{13}C NMR (100 MHz, CDCl_3) δ /ppm 151.3, 132.9, 129.0, 124.8, 120.8, 120.7, 118.7, 110.3, 86.7, 40.1, 31.9, 29.8, 23.9, 22.8, 14.2.

Compound 4a. A mixture of compound **3a** (176 mg, 0.66 mmol), *p*-toluenesulfonic acid monohydrate (76 mg, 0.40 mmol) and dry toluene (10 mL) was heated to 100°C for 1 hour. After cooling to room temperature, water was added and the product was extracted in diethyl ether. The organic phase was dried over anhydrous sodium sulfate. The solvent was removed under reduced



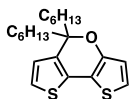
pressure and the crude product was purified by column chromatography on silica gel (dichloromethane/hexane, 1:4) to afford a green oil (135 mg, yield: 82%). ^1H NMR (400 MHz, CDCl_3) δ /ppm 7.04 (d, $J = 4.0$ Hz, 1H), 6.97 (d, $J = 4.0$ Hz, 1H), 6.72 (d, $J = 4.0$ Hz, 1H), 6.69 (d, $J = 4.0$ Hz, 1H), 1.97–1.87 (m, 4H), 0.90 (t, $J = 8.0$ Hz, 6H); ^{13}C NMR (100 MHz, CDCl_3) δ /ppm 151.5, 132.3, 129.4, 124.8, 120.8, 118.7, 110.3, 87.2, 32.4, 8.4.

Compound 4b. A mixture of compound **3b** (160 mg, 0.49 mmol), *p*-toluenesulfonic acid monohydrate (56 mg, 0.29 mmol) and dry toluene (10 mL) was heated to 100°C for 1 hour. After cooling to room temperature, water was added and the product was extracted in diethyl ether. The organic phase was dried over anhydrous sodium sulfate. The solvent was removed under reduced

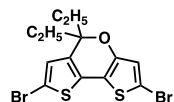


pressure and the crude product was purified by column chromatography on silica gel (dichloromethane/hexane, 1:7) to afford a green oil (132 mg, yield: 88%). ^1H NMR (400 MHz, CDCl_3) δ /ppm 7.03 (d, $J = 4.0$ Hz, 1H), 6.97 (d, $J = 4.0$ Hz, 1H), 6.71 (d, $J = 4.0$ Hz, 1H), 6.68 (d, $J = 4.0$ Hz, 1H), 1.94–1.81 (m, 4H), 1.41–1.35 (m, 2H), 1.32–1.23 (m, 6H), 0.85 (t, $J = 8.0$ Hz, 6H); ^{13}C NMR (100 MHz, CDCl_3) δ /ppm 151.3, 132.9, 129.1, 124.8, 120.8, 120.7, 118.7, 110.3, 86.7, 39.9, 26.2, 23.2, 14.2.

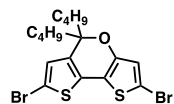
Compound 4c. A mixture of compound **3c** (180 mg, 0.55 mmol), *p*-toluensulfonic acid monohydrate (63 mg, 0.33 mmol) and dry toluene (10 mL) was heated to 100 °C for 1 hour. After cooling to room temperature, water was added and the product was extracted in diethyl ether. The organic phase was dried over anhydrous sodium sulfate. The solvent was removed under reduced pressure and the crude product was purified by column chromatography on silica gel (dichloromethane/hexane, 1:10) to afford a dark green oil (147 mg, yield: 78%). ¹H NMR (400 MHz, CDCl₃) δ/ppm 7.03 (d, *J* = 4.0 Hz, 1H), 6.97 (d, *J* = 4.0 Hz, 1H), 6.70 (d, *J* = 8.0 Hz, 1H), 6.67 (d, *J* = 8.0 Hz, 1H), 1.91–1.81 (m, 4H), 1.42–1.34 (m, 2H), 1.31–1.20 (m, 14H), 0.85 (t, *J* = 8.0 Hz, 6H); ¹³C NMR (100 MHz, CDCl₃) δ/ppm 151.3, 132.9, 129.0, 124.8, 120.8, 120.7, 118.7, 110.3, 86.7, 40.1, 31.9, 29.8, 23.9, 22.8, 14.2.



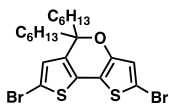
Compound 5a. A solution of compound **4a** (125 mg, 0.50 mmol) in dry DMF (10 mL) was cooled to –20 °C under nitrogen atmosphere. After that, N-bromosuccinimide (NBS) (312 mg, 1.75 mmol) was added in one portion and the solution was stirred to –20 °C for 3 hours. Then, a 0.1 M solution of sodium thiosulfate was added for quenching the reaction and the crude product was extracted in dichloromethane. The organic phase was dried over anhydrous sodium sulfate. The solvent was removed under reduced pressure and the crude product was purified by column chromatography on silica (dichloromethane/hexane, 1:4) to afford a green oil (149 mg, yield: 73%). ¹H NMR (400 MHz, CDCl₃) δ/ppm 6.67 (s, 1H), 6.65 (s, 1H), 1.94–1.78 (m, 4H), 0.89 (t, *J* = 8.0 Hz, 6H); ¹³C NMR (100 MHz, CDCl₃) δ/ppm 150.4, 132.0, 129.8, 127.5, 121.9, 110.9, 109.5, 108.2, 87.4, 32.3, 8.3.



Compound 5b. A solution of compound **4b** (122 mg, 0.40 mmol) in dry DMF (10 mL) was cooled to –20 °C under nitrogen atmosphere. After that, NBS (312 mg, 1.75 mmol) was added in one portion and the solution was stirred to –20 °C for 3 hours. Then, a 0.1 M solution of sodium thiosulfate was added for quenching the reaction and the crude product was extracted in dichloromethane. The organic phase was dried over anhydrous sodium sulfate. The solvent was removed under reduced pressure and the crude product was purified by column chromatography on silica (dichloromethane/hexane, 1:8) to afford a green oil (132 mg, yield: 71%). ¹H NMR (400 MHz, CDCl₃) δ/ppm 6.68 (s, 1H), 6.66 (s, 1H), 1.91–1.76 (m, 4H), 1.41–1.36 (m, 2H), 1.34–1.21 (m, 6H), 0.89 (t, *J* = 8.0 Hz, 6H); ¹³C NMR (100 MHz, CDCl₃) δ/ppm 150.1, 132.4, 129.2, 127.3, 121.8, 110.7, 109.3, 108.0, 87.3, 39.6, 25.9, 23.0, 14.0.

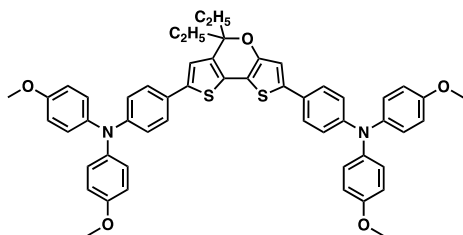


Compound 5c. A solution of compound **4c** (123 mg, 0.34 mmol) in dry DMF (10 mL) was cooled to –20 °C under nitrogen atmosphere. After that, NBS (212 mg, 1.19 mmol) was added in one portion and the solution was stirred to –20 °C for 3 hours. Then, a 0.1 M solution of sodium thiosulfate was added for quenching the reaction and the crude product was extracted in



dichloromethane. The organic phase was dried over anhydrous sodium sulfate. The solvent was removed under reduced pressure and the crude product was purified by column chromatography on silica (dichloromethane/hexane, 1:10) to afford a green oil (120 mg, yield: 68%). ^1H NMR (400 MHz, CDCl_3) δ /ppm 6.68 (s, 1H), 6.66 (s, 1H), 1.90–1.76 (m, 4H), 1.40–1.26 (m, 2H), 1.40–1.26 (m, 14H), 0.88 (t, $J = 8.0$ Hz, 6H); ^{13}C NMR (100 MHz, CDCl_3) δ /ppm 150.1, 132.5, 129.2, 127.3, 121.8, 110.7, 109.3, 108.1, 87.3, 39.7, 31.7, 29.6, 23.7, 22.7, 14.1.

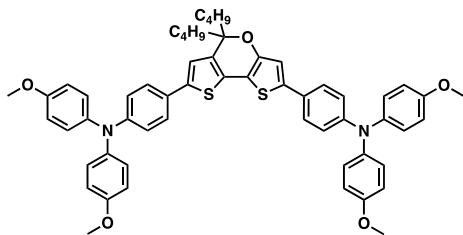
DTPA-Et. A solution of compound **5a** (152 mg, 0.37 mmol), 4-(4,4,5,5-tetramethyl-1,2,3-dioxaborolan-2-yl)-



N,N-bis(4-methoxyphenyl)-aniline (351 mg, 0.81 mmol), $\text{Pd}(\text{PPh}_3)_4$ (43 mg, 0.037 mmol) and K_3PO_4 (942 mg, 4.44 mmol) in dry DMF (8 mL) was degassed for 30 minutes. The reaction was heated to 80 °C for 2 hours. The mixture was cooled to room temperature and water was added. The resulting precipitate was

filtered and washed with water. The crude product was purified by column chromatography on silica (dichloromethane/hexane, 7:3) to afford **DTPA-Et** as an orange solid (180 mg, yield: 57%). ^1H NMR (400 MHz, $\text{THF-}d_8$) δ /ppm 7.40–7.35 (m, 4H), 7.05–7.00 (m, 9H), 6.88–6.83 (m, 13H), 3.75 (s, 12H), 2.00–1.91 (m, 4H), 0.94 (t, $J = 8.0$ Hz, 6H); ^{13}C NMR (100 MHz, $\text{THF-}d_8$) δ /ppm 157.6, 153.1, 149.7, 149.3, 141.7, 141.5, 141.0, 140.4, 133.9, 128.4, 127.8, 127.5, 127.2, 126.7, 126.4, 121.7, 121.0, 120.5, 115.7, 114.0, 109.3, 87.7, 55.8, 33.4, 8.8; FTIR (neat): 3036, 2930, 2831, 1600, 1498, 1460, 1439, 1317, 1278, 1235, 1176, 1032, 820, 594 cm^{-1} ; HRMS calcd for $\text{C}_{53}\text{H}_{48}\text{N}_2\text{O}_5\text{S}_2$ [M^+] 856.3005; found 856.3014.

DTPA-Bu. A solution of compound **5b** (119 mg, 0.26 mmol), 4-(4,4,5,5-tetramethyl-1,2,3-dioxaborolan-2-yl)-

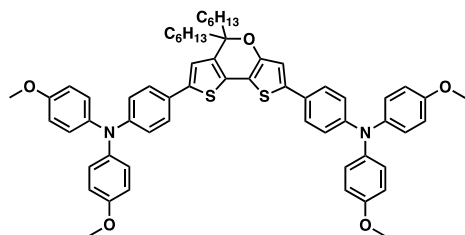


N,N-bis(4-methoxyphenyl)-aniline (247 mg, 0.57 mmol), $\text{P}(\text{PPh}_3)_4$ (30 mg, 0.026 mmol) and K_3PO_4 (662 mg, 3.12 mmol) in dry DMF (8 mL) was degassed for 30 minutes. The reaction was heated to 80 °C for 2 hours. The mixture was cooled to room temperature and water was added. The resulting precipitate was

filtered and washed with water. The crude product was purified by column chromatography on silica (dichloromethane/hexane, 1:1) to afford **DTPA-Bu** as an orange solid (140 mg, yield: 59%). ^1H NMR (400 MHz, $\text{THF-}d_8$) δ /ppm 7.39–7.35 (m, 4H), 7.05–7.01 (m, 9H), 6.88–6.83 (m, 13H), 3.75 (s, 12H), 1.96–1.92 (m, 4H), 1.48–1.27 (br, 8H), 0.87 (t, $J = 8.0$ Hz, 6H); ^{13}C NMR (100 MHz, $\text{THF-}d_8$) δ /ppm 157.6, 157.5, 153.0, 149.7, 149.3, 141.8, 141.6, 141.0, 140.4, 134.5, 128.0, 127.8, 127.6, 127.5, 127.2, 126.6, 126.4, 121.7, 121.1, 120.4, 115.7, 115.6, 114.0, 109.2, 87.1, 55.8, 41.1, 27.1, 24.1, 14.6; FTIR (neat): 3032, 2928, 2832,

1601, 1498, 1459, 1439, 1317, 1278, 1235, 1175, 1033, 821, 595 cm^{-1} ; HRMS calcd for $\text{C}_{57}\text{H}_{56}\text{N}_2\text{O}_5\text{S}_2$ [M^+] 912.3631; found 912.3621.

DTPA-Hex. A solution of compound **5c** (110 mg, 0.21 mmol), 4-(4,4,5,5-tetramethyl-1,2,3-dioxaborolan-2-



yl)-*N,N*-bis(4-methoxyphenyl)-aniline (200 mg, 0.46 mmol), $\text{Pd}(\text{PPh}_3)_4$ (30 mg, 0.021 mmol) and K_3PO_4 (535 mg, 2.52 mmol) in dry DMF (8 mL) was degassed for 30 minutes. The reaction was heated to 80 $^\circ\text{C}$ for 2 hours. The mixture was cooled to room temperature and water was added. The resulting precipitate was

filtered and washed with water. The crude product was purified by column chromatography on silica (dichloromethane/hexane, 2:1) to afford **DTPA-Hex** as an orange solid (110 mg, yield: 54%). ^1H NMR (400 MHz, $\text{THF-}d_8$) δ /ppm 7.37–7.35 (m, 4H), 7.05–7.00 (m, 9H), 6.88–6.83 (m, 13H), 3.75 (s, 12H), 1.98–1.89 (m, 4H), 1.52–1.40 (m, 4H), 1.29–1.26 (m, 12H), 0.85 (t, $J = 8.0$ Hz, 6H); ^{13}C NMR (100 MHz, $\text{THF-}d_8$) δ /ppm 157.6, 157.5, 153.0, 149.7, 149.3, 141.8, 141.6, 141.0, 140.4, 134.6, 128.0, 127.8, 127.6, 127.5, 127.2, 126.6, 126.4, 121.7, 121.1, 120.4, 115.7, 115.6, 114.0, 109.2, 87.1, 55.8, 41.3, 32.9, 30.8, 24.9, 23.7, 14.6; FTIR (neat): 2927, 2852, 2832, 1600, 1498, 1460, 1439, 1317, 1281, 1235, 1176, 1104, 1032, 821, 575, 522 cm^{-1} ; HRMS calcd for $\text{C}_{61}\text{H}_{64}\text{N}_2\text{O}_5\text{S}_2$ [M^+] 968.4257; found 968.4215.

3. Theoretical calculations

The theoretical characterization of the DTPA HTMs was done by means of density functional theory (DFT) and time-dependent DFT (TD-DFT) calculations using the τ -dependent gradient-corrected correlation BMK functional^[4] with the Pople's 6-311G(d,p)^[5,6] basis set. Solvent effects were included in the calculations by using the self-consistent reaction field approach^[7] with the solvation model based on density (SMD).^[8] Dichloromethane was the solvent used with a dielectric constant $\epsilon = 8.93$. All the calculations were performed with the Gaussian 16 suite of programs,^[9] except for the molecular volumes of the three DTPA HTMs, which were calculated using the MoloVol program,^[10] and for the electronic descriptor Λ , computed using Multiwfn 3.8, which was used to perform the charge-transfer characterization of the S_1 electronic state.^[11] The contour isovalue used to render the molecular orbitals was set at 0.03.

3.1. Structural properties

The main relevant bond angles and dihedral angles for the three minimum-energy structures calculated for the DTPA HTMs, shown in **Fig. S1**, are listed in **Table S1**.

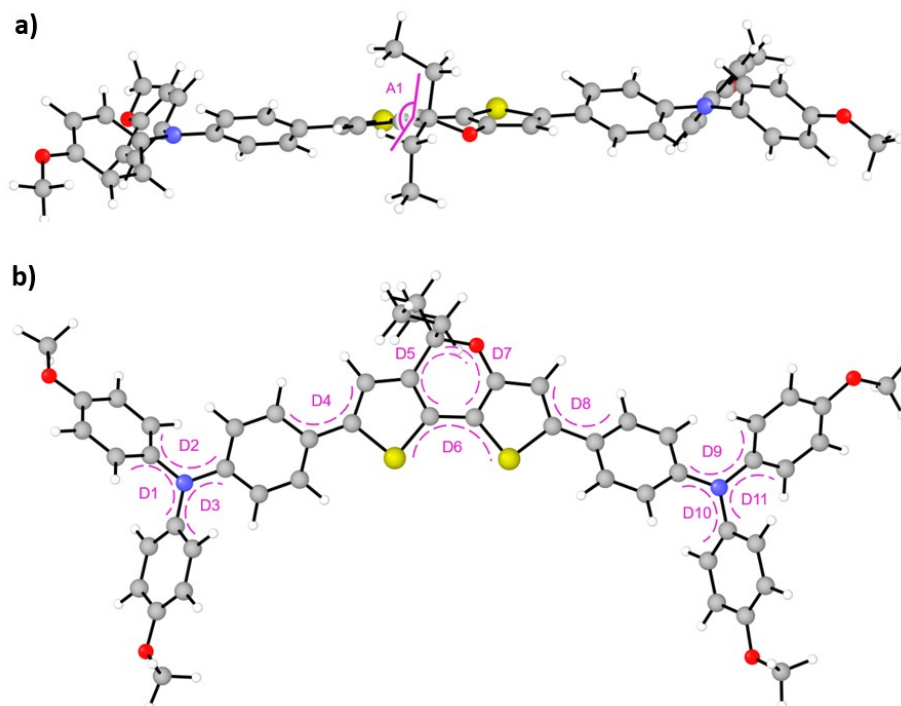


Fig. S1. Side (a) and top (b) views of the minimum-energy structure of **DTPA-Et** calculated at the BMK/6-311G(d,p) level of theory (in CH₂Cl₂). The most relevant bond angles and dihedral angles are labeled and their values for the three DTPA HTMs are listed in **Table S1**.

Table S1. Optimized BMK/6-311G(d,p) values (in degrees) calculated for the bond angles and dihedral angles defined in **Fig. S1** for **DTPA-Et**, **DTPA-Bu** and **DTPA-Hex**.

HTM	A1	D1	D2	D3	D4	D5	D6	D7	D8	D9	D10	D11
DTPA-Et	111.73	48.00	50.10	49.27	22.83	30.96	11.02	26.81	22.14	51.20	50.66	49.69
DTPA-Bu	111.79	48.23	50.00	49.94	23.66	30.99	11.23	27.05	20.58	51.46	50.38	50.02
DTPA-Hex	111.79	48.38	49.70	49.92	23.96	30.96	11.12	26.90	20.68	51.34	50.90	50.76

3.2. Frontier Molecular Orbitals (FMOs) of DTPA-Bu and DTPA-Hex

The FMOs of **DTPA-Bu** and **DTPA-Hex** are shown in **Fig. S2** and **S3**, respectively. The energies of the different FMOs for the three DTPA HTMs and spiro-OMeTAD are listed in **Table S2**.

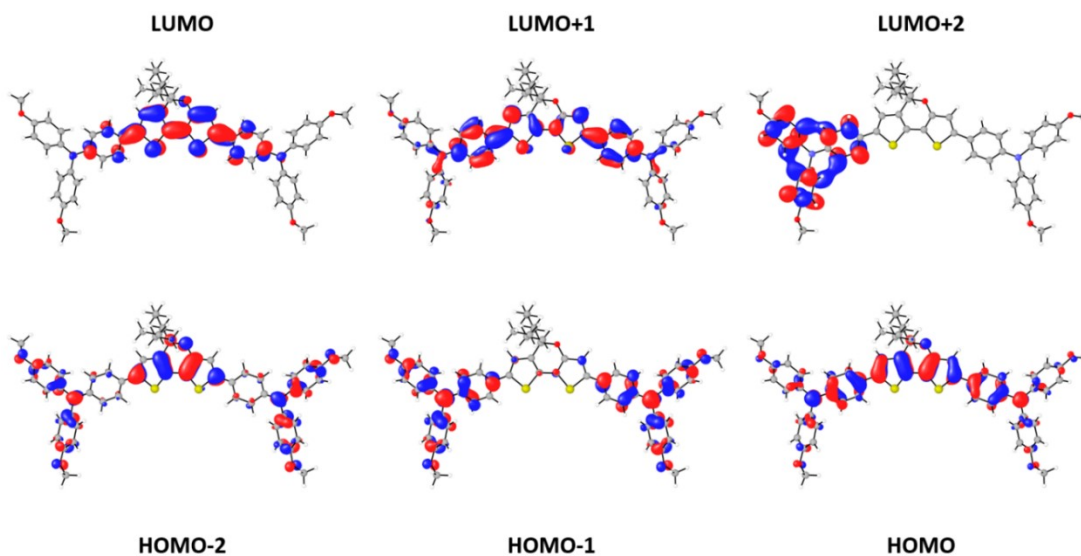


Fig. S2. Frontier molecular orbitals (FMOs) of **DTPA-Bu**. The contribution of the different FMOs to the main electronic transitions in the absorption spectrum is listed in **Table S3**.

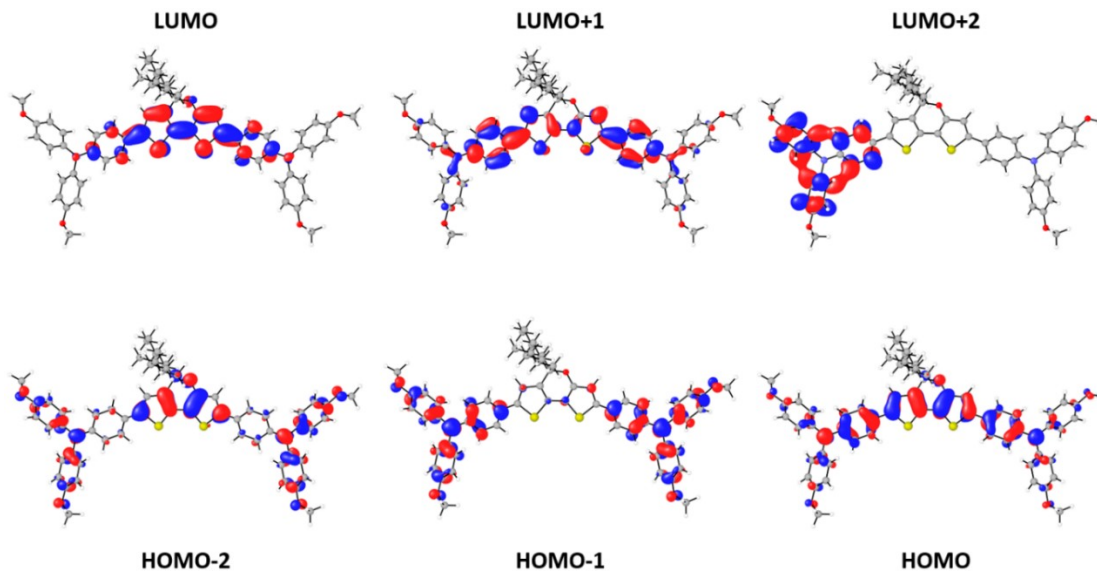


Fig. S3. Frontier molecular orbitals (FMOs) of **DTPA-Hex**. The contribution of the different FMOs to the main electronic transitions in the absorption spectrum is listed in **Table S3**.

Table S2. Energy (eV) of the frontier molecular orbitals calculated at the BMK/6-311G(d,p) level (in CH₂Cl₂) for **DTPA-Et**, **DTPA-Bu**, **DTPA-Hex** and spiro-OMeTAD. H refers to HOMO and L to LUMO.

	H-1	H-2	H	L	H+1	H+2
DTPA-Et	-6.17	-5.64	-5.22	-1.13	-0.16	-0.05
DTPA-Bu	-6.17	-5.65	-5.22	-1.13	-0.16	-0.05
DTPA-Hex	-6.17	-5.65	-5.22	-1.13	-0.16	-0.05
spiro-OMeTAD	-5.90	-5.23	-5.18	0.01	0.04	0.07

3.3. Absorption spectra

Table S3. Excitation energies (in eV and nm), oscillator strengths (*f*) and description in terms of molecular orbitals calculated at the BMK/6-311G(d,p) level of theory in CH₂Cl₂ for some of the lowest-energy singlet excited states (S_n) of **DTPA-Bu** and **DTPA-Hex**. H and L correspond to HOMO and LUMO, respectively.

State	DTPA-Bu					DTPA-Hex				
	<i>E</i> (eV)	λ (nm)	<i>f</i>	Monoexcitation	%	<i>E</i> (eV)	λ (nm)	<i>f</i>	Monoexcitation	%
S ₁	2.73	454	2.00	H → L	71	2.73	453	2.00	H → L	71
				H-1 → L+1	16				H-1 → L+1	16
				H-2 → L+1	13				H-2 → L+1	13
S ₂	3.42	363	0.25	H-1 → L	64	3.42	363	0.25	H-1 → L	64
				H → L+1	36				H → L+1	36
S ₅	3.85	322	0.24	H-2 → L	47	3.85	322	0.25	H-2 → L	54
				H-1 → L+1	22				H-1 → L+1	24
				H → L+1	22				H → L+1	12
S ₉	4.38	283	0.38	H-2 → L+7	44	4.38	283	0.39	H-2 → L+7	44
				H-1 → L+7	38				H-1 → L+7	38
				H → L+7	18				H → L+7	18

The TD-DFT-convoluted absorption spectra calculated at the BMK/6-311G(d,p) level in CH₂Cl₂ for **DTPA-Et**, **DTPA-Bu** and **DTPA-Hex**, compared to the experimental spectra, and the electronic transitions responsible of their shape are shown in **Fig. S4**, **S5** and **S6**, respectively.

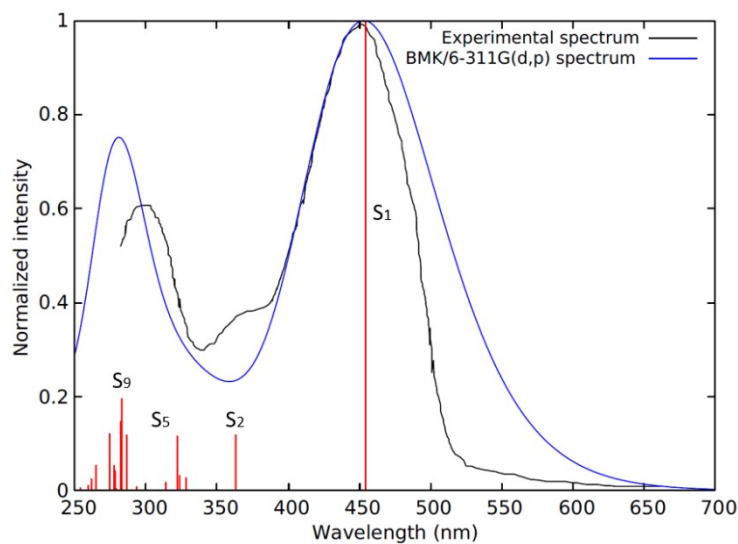


Fig. S4. Convolution of TD-DFT BMK/6-311G(d,p) (blue) and experimental (black) absorption spectra of **DTPA-Et** in CH_2Cl_2 , alongside with the singlet excited states (red) that contribute to each band of the theoretical spectrum. The height of the red bars corresponds to the normalized oscillator strength (f) of the transition to each electronic state. The non-normalized values of f are listed in **Table 2**.

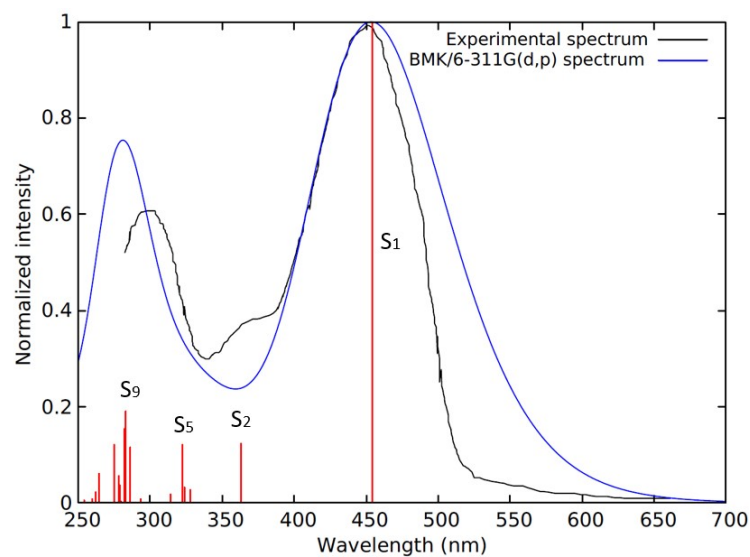


Fig. S5. Convolution of TD-DFT BMK/6-311G(d,p) (blue) and experimental (black) absorption spectra of **DTPA-Bu** in CH_2Cl_2 , alongside with the singlet excited states (red) that contribute to each band of the theoretical spectrum. The height of the red bars corresponds to the normalized oscillator strength (f) of the transition to each electronic state. The non-normalized values of f are listed in **Table S3**.

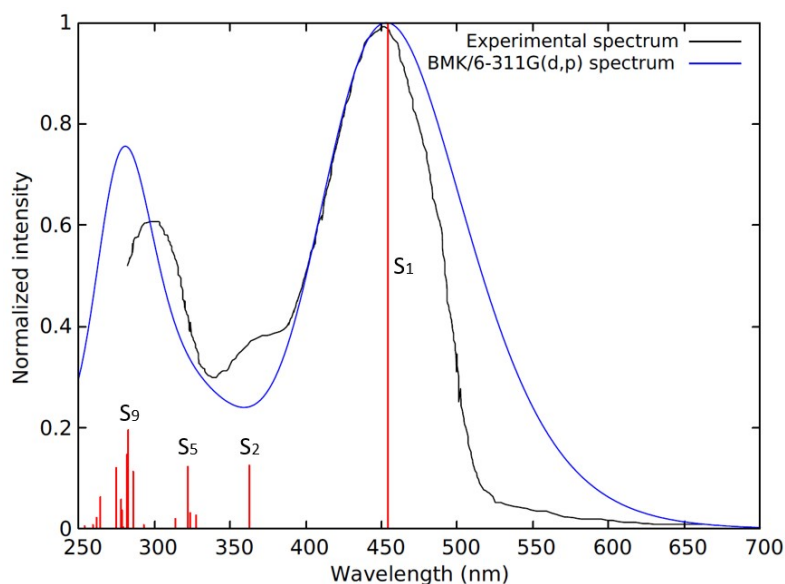


Fig. S6. Convolved TD-DFT BMK/6-311G(d,p) (blue) and experimental (black) absorption spectra of **DTPA-Hex** in CH_2Cl_2 , alongside with the singlet excited states (red) that contribute to each band of the theoretical spectrum. The height of the red bars corresponds to the normalized oscillator strength (f) of the transition to each electronic state. The non-normalized values of f are listed in **Table S3**.

The LUMO+7 molecular orbital of the three DTPA HTMs, relevant for the excitation to S_9 , is shown in **Fig. S7**. The excitation to S_9 shows a charge-transfer character, as the LUMO+7 molecular orbital is localized on a TPA unit.

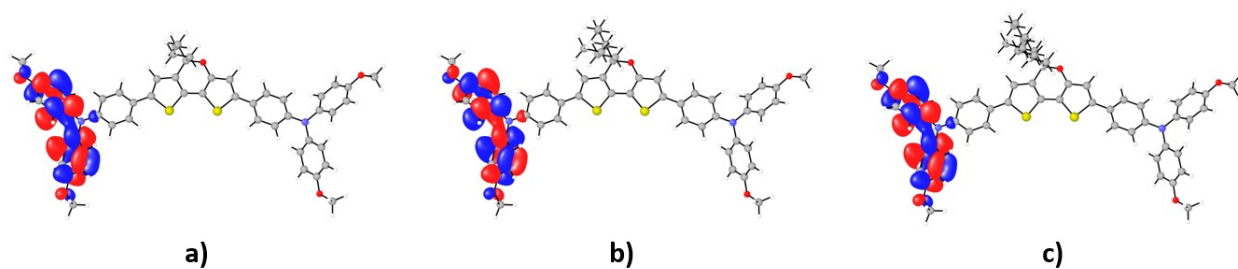


Fig. S7. LUMO+7 molecular orbital of **DTPA-Et** (a), **DTPA-Bu** (b) and **DTPA-Hex** (c).

3.4 Charge-transfer characterization of the S_1 electronic state

In order to accurately describe the nature of the S_1 electronic state for the three DTP-based HTMs, different approaches were considered. In a qualitative manner, whether an electronic transition is a local or charge-transfer excitation could be evaluated by direct inspection of the frontier molecular orbitals involved in the electronic transition (as mentioned in the text) but also by calculating the detachment/attachment density maps or the equivalent electron density difference (EDD) map. Within this approach, the atoms involved in the electron withdrawal and income upon excitation to a given excited state can be elucidated. The detachment/attachment and EDD maps calculated for the $S_0 \rightarrow S_1$ excitation of **DTPA-Et** displayed in **Fig. S8** show that there is a net, although small, electron density flux from the TPA units to the DTP core. This result highlights a non-negligible charge-transfer character of the S_1 excitation.

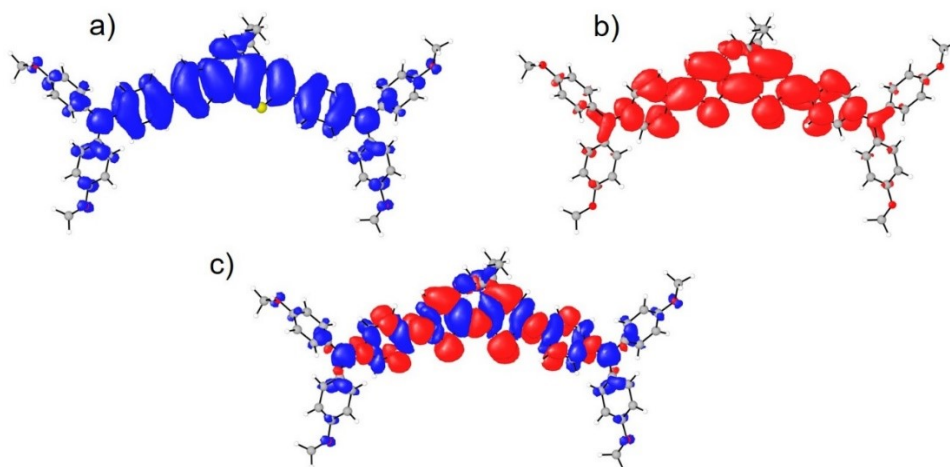


Fig. S8. Attachment (a), detachment (b) and electron density difference (EDD) (c) maps calculated for the $S_0 \rightarrow S_1$ excitation of **DTPA-Et** at the BMK/6-311G(d,p)/SMD level of theory in dichloromethane. Blue and red colors indicate the electron density withdrawal and accumulation, respectively.

As an alternative approach to evaluate the CT character of S_1 , the total Mulliken charges accumulated by the different fragments constituting the molecules were calculated. In the S_0 ground state, the three DTPA molecules concentrate a negative charge of $-0.22e$ on the DTP core owing to the electron-density transfer from the electron-donor TPA units ($+0.22e$). In passing to S_1 , the total charge of the DTP core increases to $-0.31e$ due to an additional charge transfer mainly from the external phenyl rings of the TPA units. However, this additional charge transfer is not reflected in the electric dipole moments of the molecules, which remain mainly unchanged in passing from S_0 (**DTPA-Et**: 3.30 D, **DTPA-Bu**: 3.27 D, **DTPA-Hex**: 3.31 D) to S_1 (**DTPA-Et**: 3.09 D, **DTPA-Bu**: 3.17 D, **DTPA-Hex**: 3.24 D) due to the almost symmetrical structure of the molecules. This justifies that TD-DFT calculations predict only a small shift from 454 nm (2.73 eV) in

dichloromethane ($\epsilon = 8.93$) to 442 nm (2.81 eV) in more polar ethanol ($\epsilon = 32.61$). Therefore, no relevant solvatochromism should be expected for the band associated to the S_1 excitation.

To obtain a more quantitative estimation of the charge-transfer character of the $S_0 \rightarrow S_1$ electronic transition, the electronic descriptor Λ was employed.^[12] Λ essentially measures the overlap between the occupied and unoccupied molecular orbitals that are involved in a given electronic excitation, ranging from 1 (local excitation) to 0 (CT excitation). The value of Λ computed for the $S_0 \rightarrow S_1$ transition is 0.72 for all the three DTP-based HTMs. As stated in the main text, this value highlights a moderate CT character of the excitation, although it should be mainly described as a short-range transition.

3.5. Mulliken charges analysis for ionization processes

The Mulliken net charges accumulated by the three fragments in which the DTP-based HTMs are divided (**Fig. S8**) are listed in **Table S4** for the radical cation, singlet dication and radical trication.

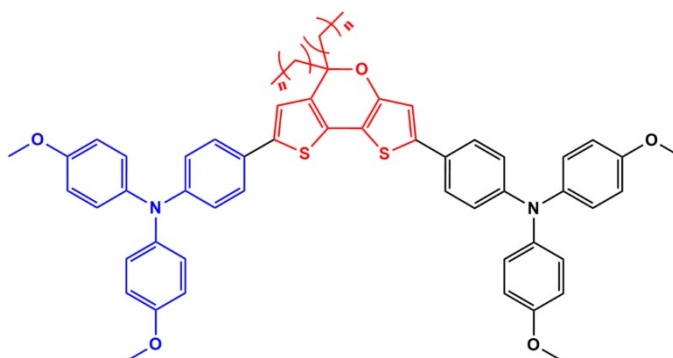


Fig. S9. Molecular fragments used to analyze the Mulliken net charges calculated for the ionized DTPA HTMs. Fragments 1 (blue) and 3 (black) correspond to the TPA units, and fragment 2 to the DTP central core.

Table S4. Mulliken charges (e) accumulated by the molecular fragments described in **Fig. S9** for the three DTPA HTMs.

	DTPA-Et			DTPA-Bu			DTPA-Hex		
	Frag. 1	Frag. 2	Frag. 3	Frag. 1	Frag. 2	Frag. 3	Frag. 1	Frag. 2	Frag. 3
Neutral	0.118	-0.218	0.099	0.099	-0.218	0.119	0.097	-0.219	0.121
Cation	0.343	0.242	0.416	0.408	0.247	0.345	0.398	0.247	0.355
Dication	0.655	0.545	0.801	0.802	0.550	0.648	0.788	0.555	0.658
Trication	1.209	0.587	1.204	1.206	0.585	1.210	1.202	0.598	1.201

3.6. Cation reorganization energies

The reorganization energies (λ_h) for the three DTPA HTMs and for spiro-OMeTAD were computed at the BMK/6-311G(d,p) level of theory in gas phase as

$$\lambda_h = \lambda_1 + \lambda_2 = (E_N^{+1} - E_C^{+1}) + (E_C^0 - E_N^0)$$

where E_X^Y is the energy of the neutral ($Y = 0$) or the cation ($Y = +1$) species at the neutral ($X = N$) or the cation ($X = C$) molecular structure.

4. Thermal properties

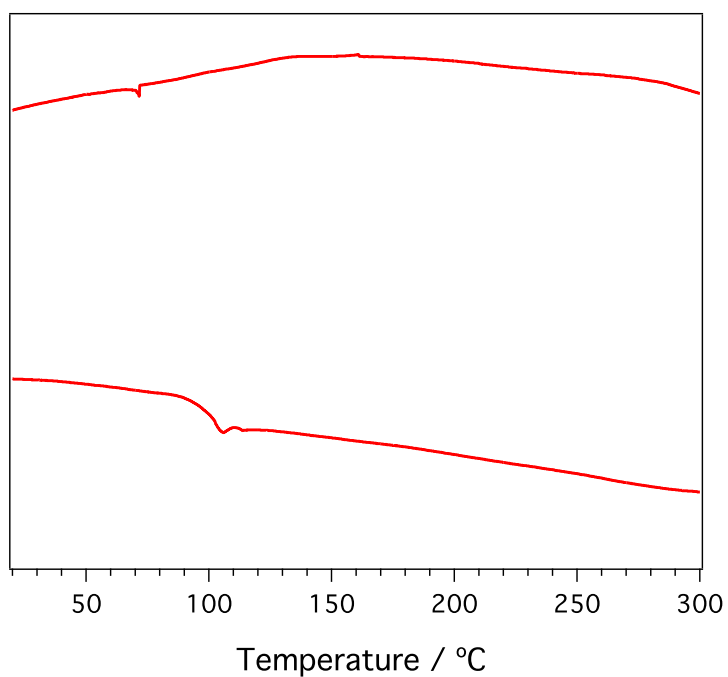


Fig. S10. DSC of **DTPA-Et** at a scan rate of 20 °C min⁻¹.

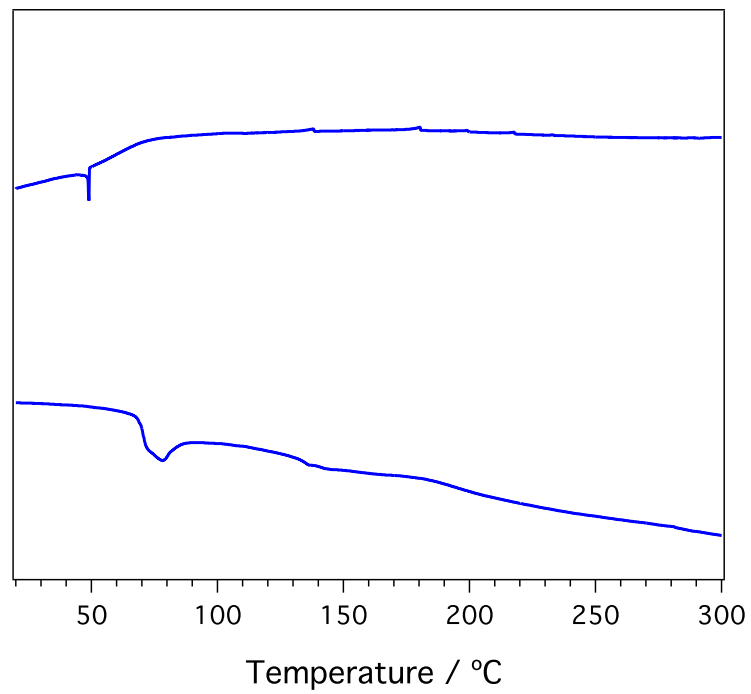


Fig. S11. DSC of **DTPA-Bu** at a scan rate of 20 °C min⁻¹.

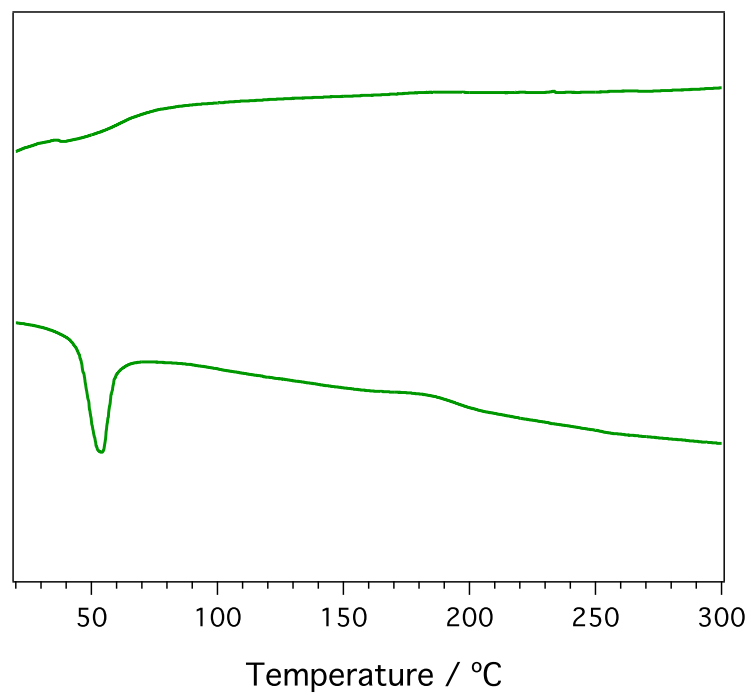


Fig. S12. DSC of **DTPA-Hex** at a scan rate of 20 °C min⁻¹.

5. Device fabrication

Standard planar solar cell devices were fabricated onto conductive ITO-coated glass substrates. The conductive substrates were cut and cleaned by sequential treatment with a 2% aqueous Helmanex solution, deionized water and isopropanol in an ultrasonic bath for 20 minutes, respectively, followed by a 15 minutes UV-ozone (UVO) exposure. Then, over the substrates, a thin layer of SnO₂ was spin-coated from a precursor solution in water (2.67 %) at 3000 rpm for 30 s, annealed in ambient air at 150 °C for 30 min and then cleaned by UVO again for 15 min. The [(FAPbI₃)_{0.87}(MAPbBr₃)_{0.13}]_{0.92}[CsPbI₃]_{0.08} perovskite was applied by spin-coating a precursor solution consisting of 548.6 mg of PbI₂ (TCI), 57.0 mg of PbBr₂ (TCI), 178.9 mg of formamidinium iodide (Dyesol), 27.02 mg of CsI and 17.41 mg of methylammonium bromide (Dyesol) dissolved in a 1:3.5 mixture of DMSO:DMF. The perovskite solution was spun at 2000 rpm for 12 s and 5000 for 30 s. 15 s prior to the end of the spin-coating sequence, 100 μL of chlorobenzene were poured onto the spinning substrate. Afterwards, the substrates were transferred onto a heating plate and annealed at 100 °C for 1 h. The hole-transporting materials were spin-coated from solutions at 5000 rpm for 30 s. The hole-transporters were dissolved in chlorobenzene with an optimized concentration of 40 mM for all DTPA-based HTMs and 60 mM spiro-OMeTAD as reference. Tert-butylpyridine (tBP), tris(2-(1H-pyrazol-1-yl)-4-tert-butylpyridine)cobalt(III) (FK-209) and tris(bis(trifluoromethylsulfonyl)imide) (Li-TFSI) were added. Equimolar amounts of additives were added for all hole-transporters: 330 mol % tBP, 50 mol % Li-TFSI from a 1.8 M stock solution in acetonitrile and 6 mol % FK-209 from a 0.25 M stock solution in acetonitrile. For the electrode, 80 nm of gold was thermally evaporated under high vacuum.

5.1 Solar Cell Characterization

The photovoltaic device performance was analyzed in air under AM 1.5G (100W cm⁻²) simulated sunlight using a potentiostat (Keithley). The light intensity was calibrated with an NREL certified KG5 filtered Si reference diode. The solar cells were masked with a metal aperture of 0.16 cm² to define the active area. The density current-voltage curves were recorded scanning at 10 mV s⁻¹. High resolution cross-section images of the finished devices were recorded with a ZEISS Merlin HR-SEM scanning electron microscope.

5.2 Energy diagram of the different constituents of the PSCs

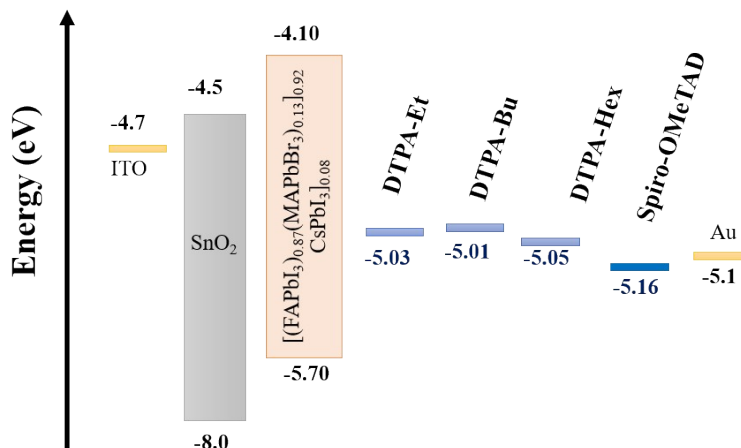


Fig. S13. Schematic energy diagram of the different layers constituting the device.

5.3 Cross-section SEM images of fabricated PSCs

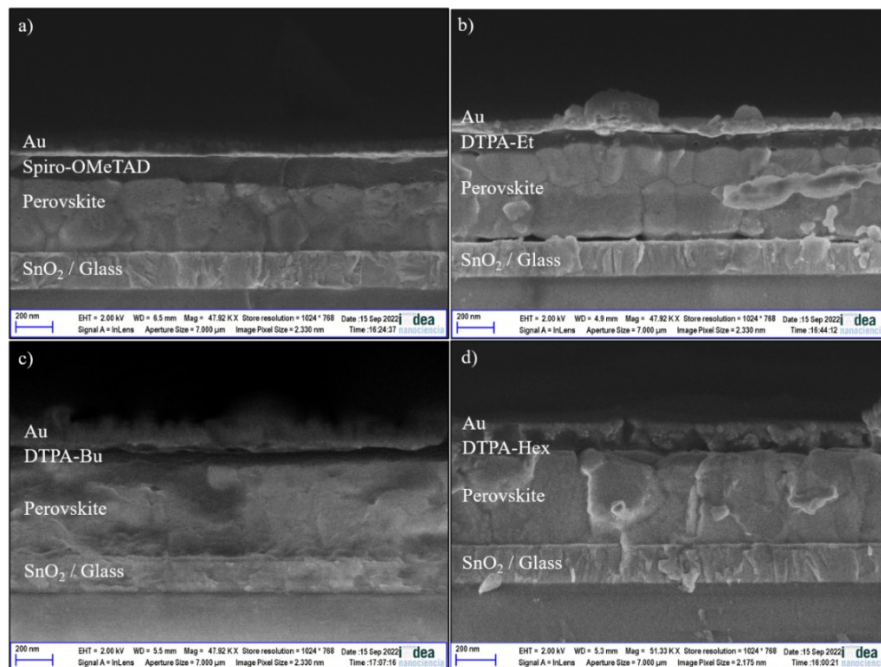


Fig. S14. Cross-section SEM images of fabricated planar PSCs incorporating as HTMs: a) spiro-OMeTAD, b) DTPA-Et, c) DTPA-Bu and d) DTPA-Hex.

5.4 Surface images

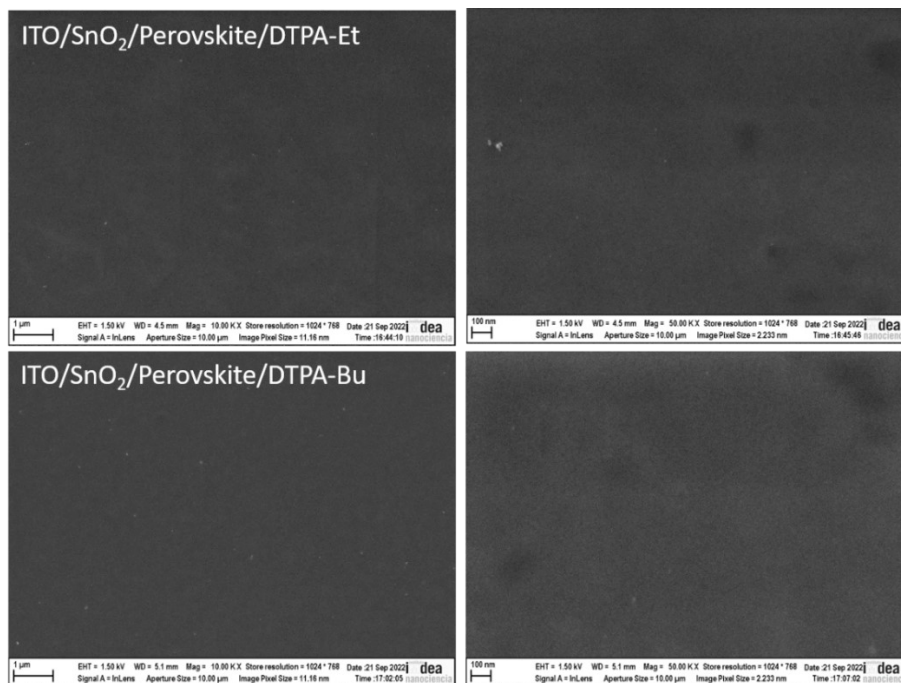


Fig. S15. Surface images of the ITO/SnO₂/Perovskite/HTM with HTMs **DTPA-Et** (top) and **DTPA-Bu** (bottom).

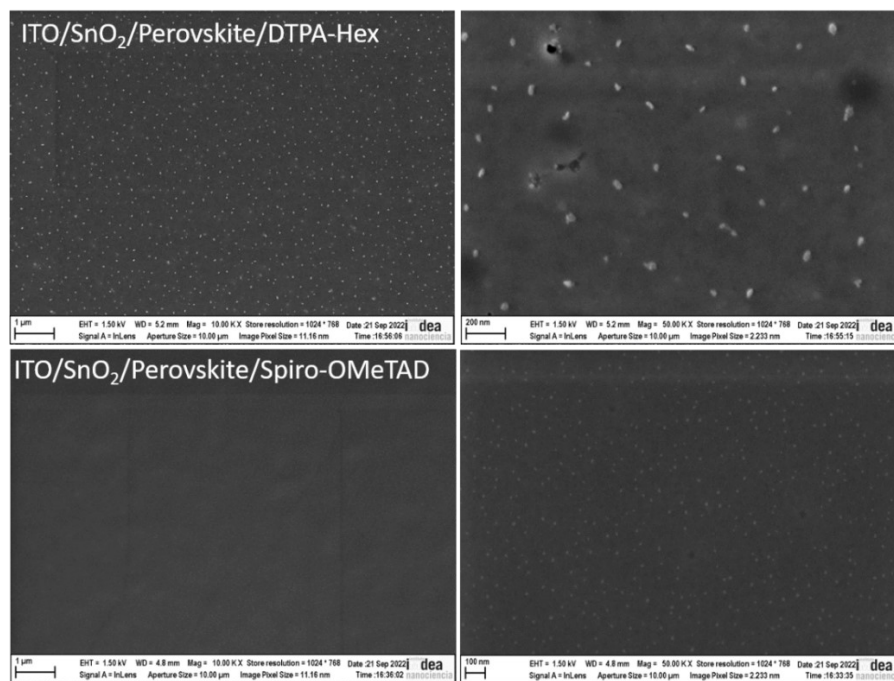


Fig. S16. Surface image of the ITO/SnO₂/Perovskite/HTM with HTMs **DTPA-Hex** (top) and **spiro-OMeTAD** (bottom).

5.5 Hysteresis curves

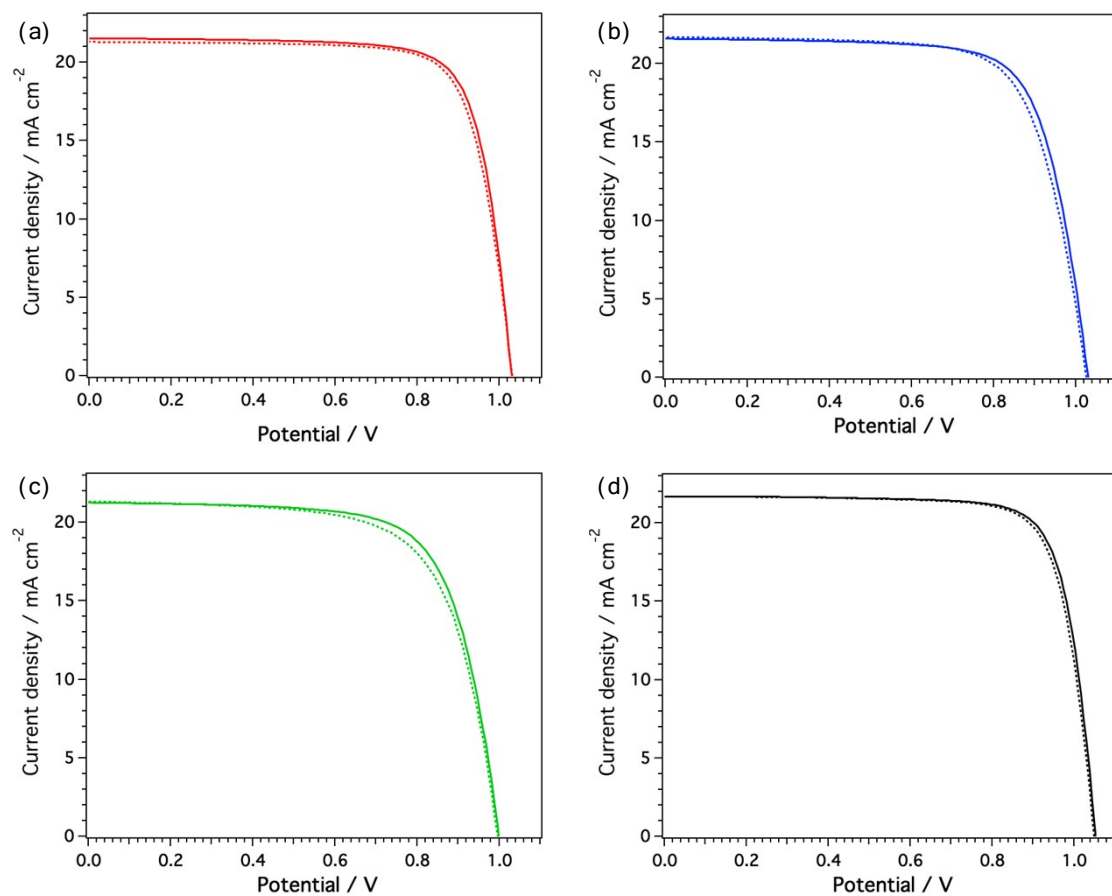


Fig. S17. Hysteresis curves for devices incorporating **DTPA-Et** (a), **DTPA-Bu** (b), **DTPA-Hex** (c), and **spiro-OMeTAD** (d) measured at 10 mV s⁻¹.

5.6 Device statistics

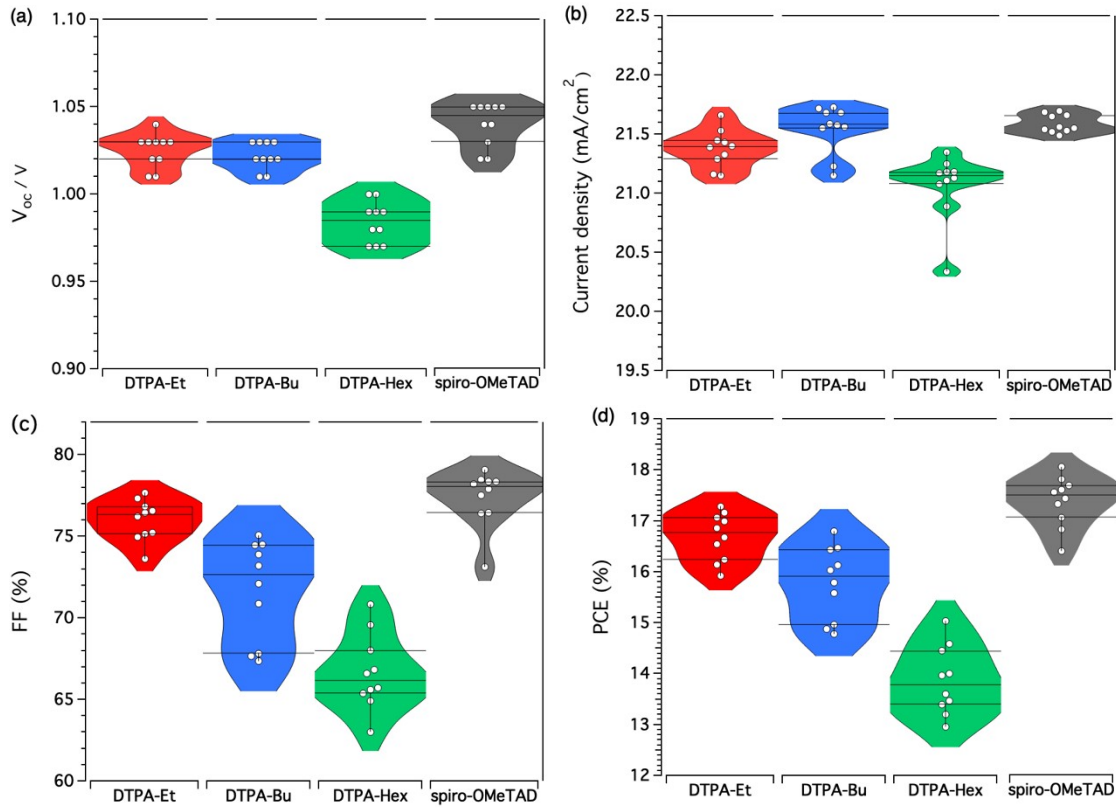


Fig. S18. Box plots of the (a) V_{OC} , (b) J_{SC} , (c) FF and (d) PCE of 10 devices with the different DTPA-based HTMs and spiro-OMeTAD.

Table S5. Statistic parameters of 10 devices of different DTPA-based HTMs and spiro-OMeTAD.

HTM	V_{OC} (V)	J_{SC} (mA cm ⁻²)	FF (%)	PCE (%)
DTPA-Et	1.03 ± 0.01	21.38 ± 0.16	76.01 ± 1.25	16.69 ± 0.47
DTPA-Bu	1.02 ± 0.01	21.55 ± 0.20	71.70 ± 3.07	15.79 ± 0.72
DTPA-Hex	0.98 ± 0.01	21.07 ± 0.28	66.66 ± 2.30	13.87 ± 0.67
spiro-OMeTAD	1.04 ± 0.01	21.59 ± 0.08	77.40 ± 1.73	17.39 ± 0.49

5.7 Stability measurements

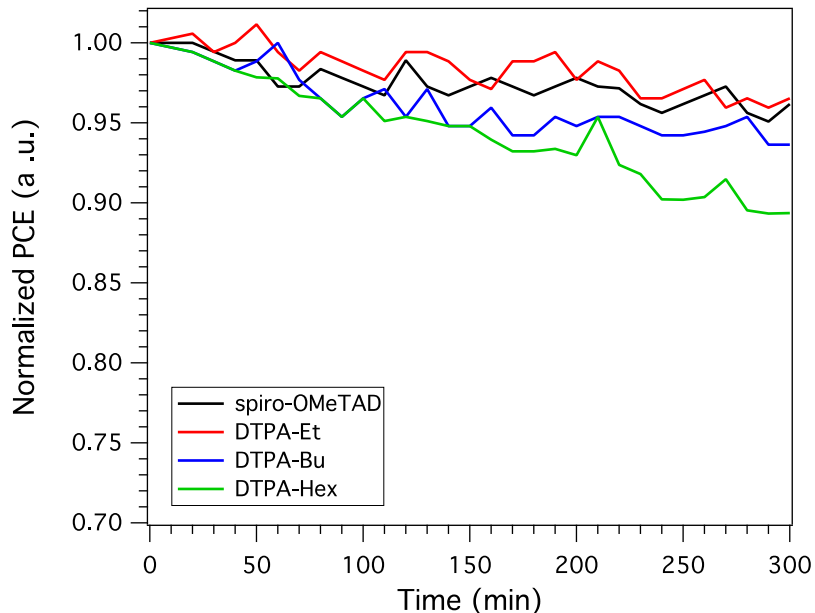


Fig. S19. Normalized efficiency vs. time at room temperature (RH 30 % in air) of perovskite-based devices using spiro-OMeTAD, **DTPA-Et**, **DTPA-Bu** and **DTPA-Hex** as HTMs.

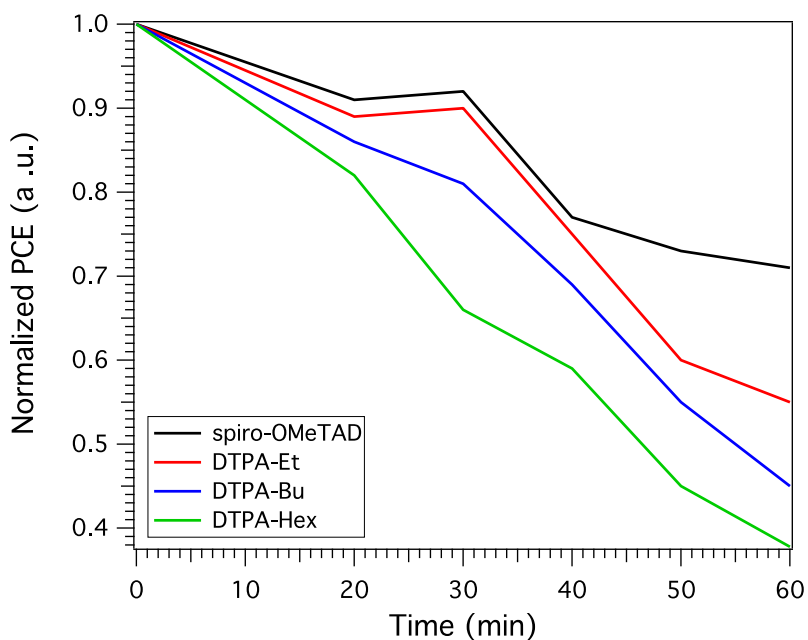


Fig. S20. Normalized efficiency vs. time at 60 °C (RH 30 % in air) of perovskite-based devices using spiro-OMeTAD, **DTPA-Et**, **DTPA-Bu** and **DTPA-Hex** as HTMs.

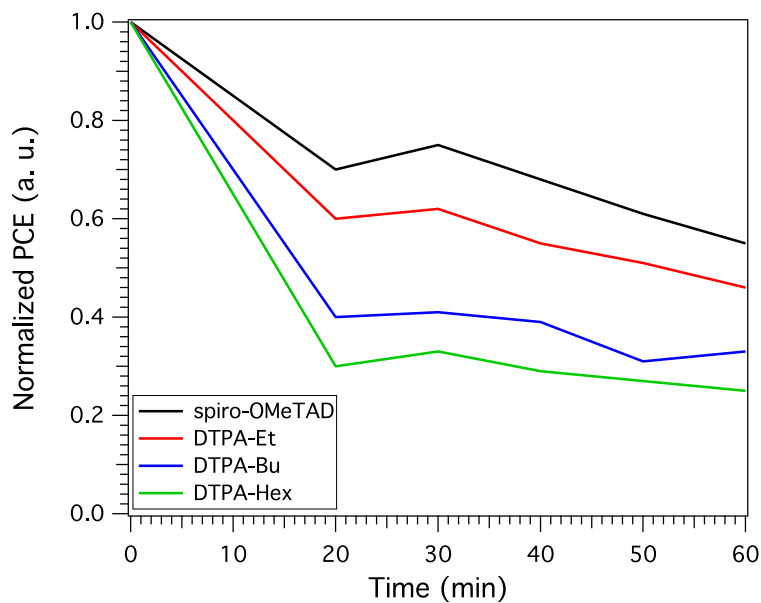


Fig. S21. Normalized efficiency vs. time at 85 °C (RH 30 % in air) of perovskite-based devices using spiro-OMeTAD, **DTPA-Et**, **DTPA-Bu** and **DTPA-Hex** as HTMs.

5.8 Hole mobility measurements

Hole mobility was measured on hole-only devices with the structure of glass/ITO/PEDOT:PSS/HTM/Au using the space-charge limited current (SCLC) method according to previous literature.^[13] The mobility was obtained fitting the SCLC curve.^[13] The applied bias was measured from 0 to 5 V.

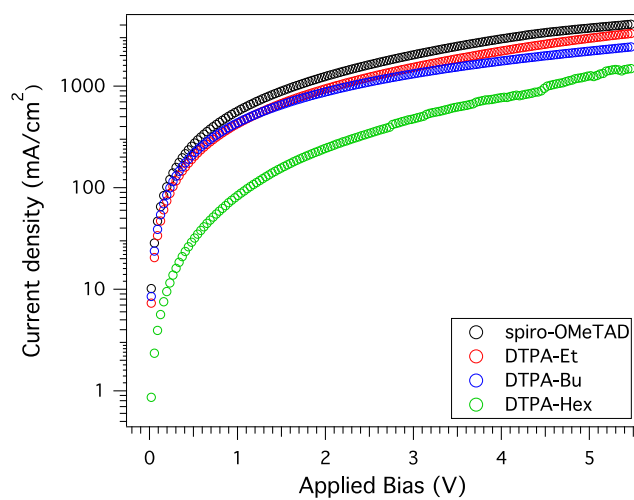


Fig. S22. J - V plots of hole-only devices based on **DTPA-Et**, **DTPA-Bu**, **DTPA-Hex** and spiro-OMeTAD.

Table S6. Hole mobilities measured for the DTPA HTMs and the reference spiro-OMeTAD.

HTM	μ (cm ² V ⁻¹ s ⁻¹)
DTPA-Et	2.53×10^{-4}
DTPA-Bu	1.11×10^{-4}
DTPA-Hex	7.41×10^{-5}
spiro-OMeTAD	4.41×10^{-4}

6. Synthetic cost for the preparation of DTPA HTMs

Synthesis of TPA-BPin			
Reagent	Price of chemical	Quantity used	Total price (€)
Aniline (Acros)	5 L / 143.10 €	1 mL	0,03
4-Iodoanisole (Acros)	500 g / 261.3 €	5,27 g	2,75
Pd ₂ (dba) ₃ (Thermo Sci.)	5g / 207 €	246 mg	10,18
Xphos (BLD Pharm.)	100 g / 139 €	255 mg	0,35
^t BuONa (Acros)	500g / 148 €	3,096 g	0,92
Toluene (Scharlab)	25 L / 480 €	30 mL	0,58
Purification (silica gel + solvents)			1,77
			16,58
	<i>Product obtained</i>	2,56 g (Yield 79%)	6,48 € / g
TPA	1 g / 6,48 €	3 g	19,44
I ₂ (Thermo Sci.)	1000 g / 250 €	0,982 g	0,25 €
H ₅ IO ₆ (Thermo Sci.)	500g / 222,30 €	0,48 g	0,26 €
EtOH (Scharlab)	25 L / 240 €	35 mL	0,34 €
Purification (silica gel + solvents)			1,77 €
			22,06 €
	<i>Product obtained</i>	3,07 g (Yield 72%)	7,19 € / g
TPA-I	1 g / 7,19 €	2,25 g	16,18 €
Bis(pinacolato)diboro	25 g / 150 €	1,99 g	11,94 €

n (Thermo Sci.)			
KOAc (Sigma-Aldrich)	500 g / 31,60 €	1,54 g	0,10 €
Pd₂(Cl₂(dppf)₂ (Fluorochem)	5 g / 112 €	0,42 g	9,41 €
DMF (Scharlab)	2,5 L / 106 €	30 mL	1,27 €
Purification (silica gel + solvents)			1,77 €
			40,67 €
	<i>Product obtained</i>	1,76 g (Yield 78%)	23,11 € / g

Synthesis of DTPA-Et

Reagent	Price of chemical	Quantity used	Total price (€)
3,3'-Dibromo-2,2'-bithiophene (BLD Pharm)	25 g / 166 €	3,70 g	24,57 €
n-Butyllithium (1,6 M in hexane) (Thermo Sci.)	500 mL / 107,23 €	15,7 mL	3,37 €
DMF (Scharlab)	2,5 L / 106 €	1,2 mL	0,05 €
Diethyl ether	5 L / 205 €	50 mL	2,05 €
Purification (silica gel + solvents)			1,77
			31,81 €
	<i>Product obtained</i>	1,72 g (Yield 78%)	18,49 € / g
Compound 1	1 g / 18,49 €	2 g	36,98 €

NaBO₃ (Thermo Sci.)	250 g / 77,50 €	3,11 g	0,96 €
CF₃CO₂H (Thermo Sci.)	100 mL / 19,55 €	10 mL	1,96 €
CHCl₃ (Thermo Sci.)	2,5 L / 14,76 €	30 mL	0,18 €
Purification (silica gel + solvents)			1,77 €
			41,85 €
	<i>Product obtained</i>	0,82 g (Yield 38%)	51,03 € / g
Compound 2	1 g / 51,03 €	0,60 g	30,62 €
Ethylmagnesium bromide (3 M in diethyl ether) (Thermo Sci.)	100 mL / 79,66 €	1,92 mL	1,53 €
THF (Scharlab)	5 L / 388 €	20 mL	1,55 €
Purification (silica gel + solvents)			1,77 €
			35,47 €
	<i>Product obtained</i>	0,63 g (Yield 81%)	56,30 € / g
Compound 3a	1 g / 56,30 €	1,1 g	61,93 €
p-Toluenesulfonic acid (Thermo Sci.)	250 g / 27,20 €	0,53 g	0,06 €
Toluene (Scharlab)	25 L / 480 €	30 mL	0,58 €
Purification (silica gel + solvents)			1,77 €
			64,34 €
	<i>Product obtained</i>	0,84 g (Yield 82%)	76,59 € / g

Compound 4a	1 g / 76,59 €	0,80 g	61,27 €
NBS (Thermo Sci.)	1 kg / 131 €	1,27 g	0,17 €
DMF (Scharlab)	2,5 L / 106 €	20 mL	0,85 €
Purification (silica gel + solvents)			1,77 €
			64,06 €
	<i>Product obtained</i>	1,02 g (Yield 78%)	62,80 € / g
Compound 5a	1 g / 62,80 €	0,25 g	15,70 €
TPA-Bpin	1 g / 23,11 €	0,58 g	13,40 €
Pd(PPh₃)₄ (Thermo Sci.)	5 g / 129,77 €	0,072 g	1,87 €
K₃PO₄ (Thermo Sci.)	1 kg / 78,48 €	1,57 g	0,12 €
DMF (Scharlab)	2,5 L / 106 €	10 mL	0,42 €
Purification (silica gel + solvents)			1,77 €
			33,28 €
	<i>Product obtained</i>	0,30 g (Yield 57%)	110,93 € / g

Synthesis of DTPA-Bu			
Reagent	Price of chemical	Quantity used	Total price (€)
3,3'-Dibromo-2,2'-bithiophene (BLD Pharm)	25 g / 166 €	3,70 g	24,57 €
n-Butyllithium (1,6 M in hexane) (Thermo Sci.)	500 mL / 107,23 €	15,7 mL	3,37 €
DMF (Scharlab)	2,5 L / 106 €	1,2 mL	0,05 €
Diethyl ether	5 L / 205 €	50 mL	2,05 €
Purification (silica gel + solvents)			1,77

			31,81 €
	<i>Product obtained</i>	1,72 g (Yield 78%)	18,49 € / g
Compound 1	1 g / 18,49 €	2 g	36,98 €
NaBO₃ (Thermo Sci.)	250 g / 77,50 €	3,11 g	0,96 €
CF₃CO₂H (Thermo Sci.)	100 mL / 19,55 €	10 mL	1,96 €
CHCl₃ (Thermo Sci.)	2,5 L / 14,76 €	30 mL	0,18 €
Purification (silica gel + solvents)			1,77 €
			41,85 €
	<i>Product obtained</i>	0,82 g (Yield 38%)	51,03 € / g
Compound 2	1 g / 51,03 €	0,60 g	30,62 €
Butylmagnesium chloride (2 M in THF) (Sigma-Aldrich)	100 mL / 76,60 €	4,32 mL	3,31 €
THF (Scharlab)	5 L / 388 €	20 mL	1,55 €
Purification (silica gel + solvents)			1,77 €
			37,25 €
	<i>Product obtained</i>	0,72 g (Yield 77%)	51,75 € / g
Compound 3b	1 g / 51,75 €	0,70 g	36,23 €
p-Toluenesulfonic acid (Thermo Sci.)	250 g / 27,20 €	0,25 g	0,03 €
Toluene (Scharlab)	25 L / 480 €	30 mL	0,58 €
Purification (silica gel + solvents)			1,77 €
			38,61 €
	<i>Product obtained</i>	0,58 g (Yield 88%)	66,57 € / g
Compound 4b	1 g / 66,57 €	0,55 g	36,61 €
NBS (Thermo Sci.)	1 kg / 131 €	1,12 g	0,15 €
DMF (Scharlab)	2,5 L / 106 €	20 mL	0,85 €
Purification (silica gel + solvents)			1,77 €
			39,38 €
	<i>Product obtained</i>	0,59 g (Yield 71%)	66,75 € / g
Compound 5b	1 g / 66,75 €	0,20 g	13,35 €
TPA-Bpin	1 g / 23,11 €	0,42 g	9,71 €
Pd(PPh₃)₄ (Thermo Sci.)	5 g / 129,77 €	0,050 g	1,30 €
K₃PO₄ (Thermo Sci.)	1 kg / 78,48 €	1,11 g	0,09 €
DMF (Scharlab)	2,5 L / 106 €	10 mL	0,42 €
Purification (silica gel + solvents)			1,77 €
			26,64 €
	<i>Product obtained</i>	0,23 g (Yield 59%)	115,83 € / g

Synthesis of DTPA-Hex			
Reagent	Price of chemical	Quantity used	Total price (€)
3,3'-Dibromo-2,2'-bithiophene (BLD Pharm)	25 g / 166 €	3,70 g	24,57 €
n-Butyllithium (1,6 M in hexane) (Thermo Sci.)	500 mL / 107,23 €	15,7 mL	3,37 €
DMF (Scharlab)	2,5 L / 106 €	1,2 mL	0,05 €
Diethyl ether	5 L / 205 €	50 mL	2,05 €
Purification (silica gel + solvents)			1,77
			31,81 €
	<i>Product obtained</i>	1,72 g (Yield 78%)	18,49 € / g
Compound 1	1 g / 18,49 €	2 g	36,98 €
NaBO₃ (Thermo Sci.)	250 g / 77,50 €	3,11 g	0,96 €
CF₃CO₂H (Thermo Sci.)	100 mL / 19,55 €	10 mL	1,96 €
CHCl₃ (Thermo Sci.)	2,5 L / 14,76 €	30 mL	0,18 €
Purification (silica gel + solvents)			1,77 €
			41,85 €
	<i>Product obtained</i>	0,82 g (Yield 38%)	51,03 € / g
Compound 2	1 g / 51,03 €	0,50 g	30,62 €
Hexylmagnesium bromide (2 M in diethyl ether) (Sigma-Aldrich)	100 mL / 69,20 €	3,60 mL	2,49 €
THF (Scharlab)	5 L / 388 €	20 mL	1,55 €
Purification (silica gel + solvents)			1,77 €
			36,43 €
	<i>Product obtained</i>	0,64 g (Yield 77%)	56,92 € / g
Compound 3c	1 g / 56,92 €	0,60 g	34,15 €
p-Toluenesulfonic acid (Thermo Sci.)	250 g / 27,20 €	0,21 g	0,02 €
Toluene (Scharlab)	25 L / 480 €	30 mL	0,58 €
Purification (silica gel + solvents)			1,77 €
			36,52 €
	<i>Product obtained</i>	0,44 g (Yield 78%)	83,02 € / g
Compound 4c	1 g / 83,02 €	0,40 g	33,21 €
NBS (Thermo Sci.)	1 kg / 131 €	0,69 g	0,09 €

DMF (Scharlab)	2,5 L / 106 €	20 mL	0,85 €
Purification (silica gel + solvents)			1,77 €
			35,92 €
	<i>Product obtained</i>	0,33 g (Yield 68%)	108,85 € / g
Compound 5c	1 g / 108,85 €	0,20 g	21,77 €
TPA-Bpin	1 g / 23,11 €	0,40 g	9,24 €
Pd(PPh₃)₄ (Thermo Sci.)	5 g / 129,77 €	0,055 g	1,43 €
K₃PO₄ (Thermo Sci.)	1 kg / 78,48 €	1,15 g	0,09 €
DMF (Scharlab)	2,5 L / 106 €	10 mL	0,42 €
Purification (silica gel + solvents)			1,77 €
			34,72 €
	<i>Product obtained</i>	0,20 g (Yield 54%)	173,60 € / g

7. Supplementary figures

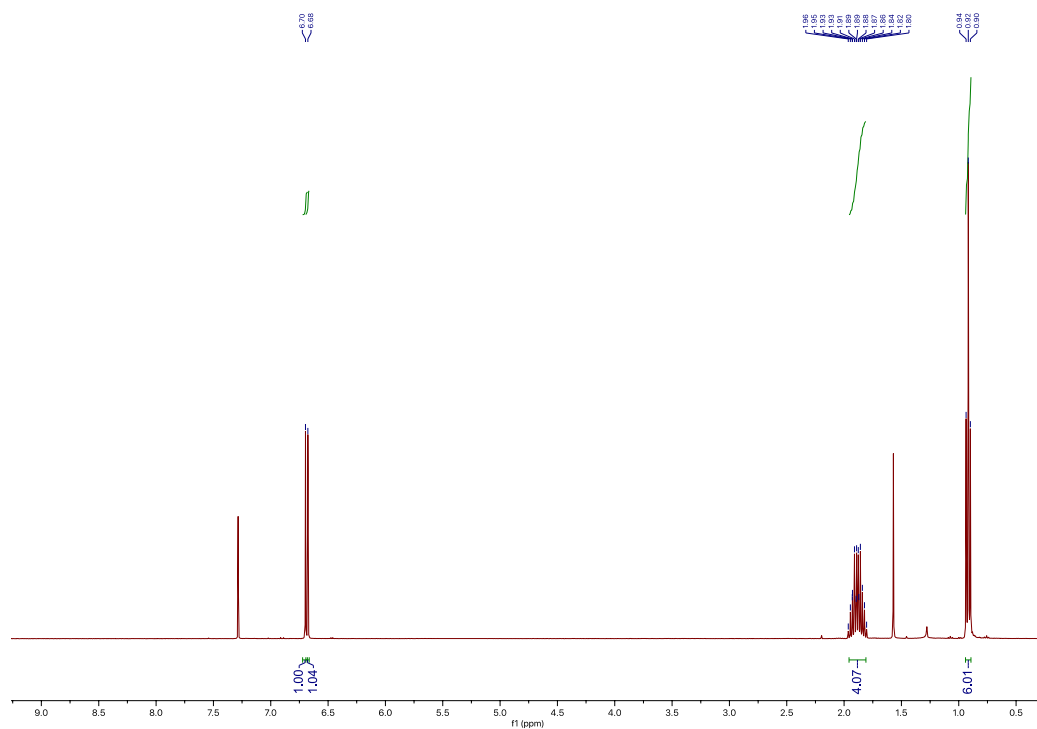


Fig. S23. ¹H NMR (400 MHz, CDCl₃, 298 K) of compound **5a**.

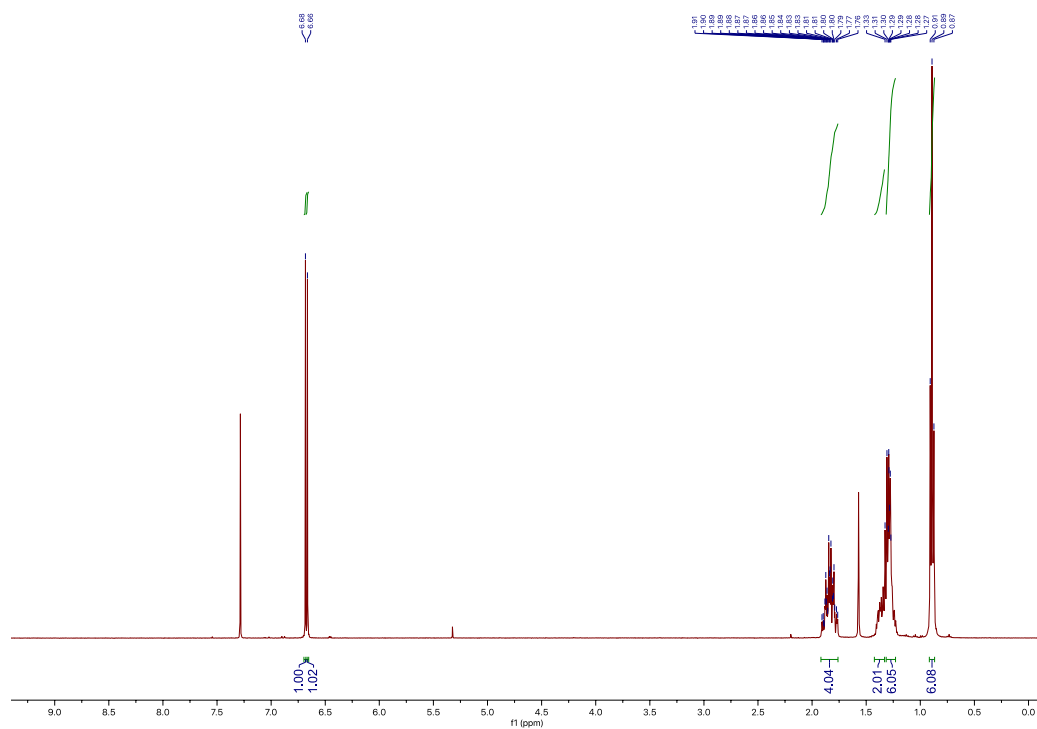


Fig. S24. ¹H NMR (400 MHz, CDCl₃, 298 K) of compound **5b**.

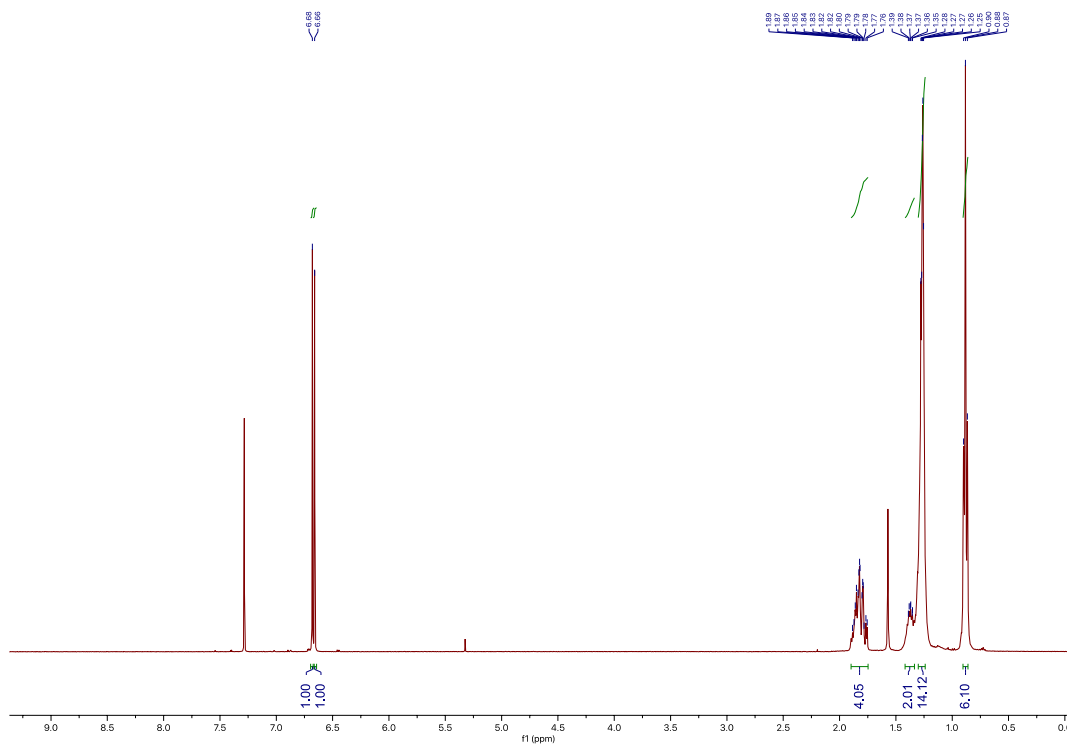


Fig. S25. ^1H NMR (400 MHz, CDCl_3 , 298 K) of compound **5c**.

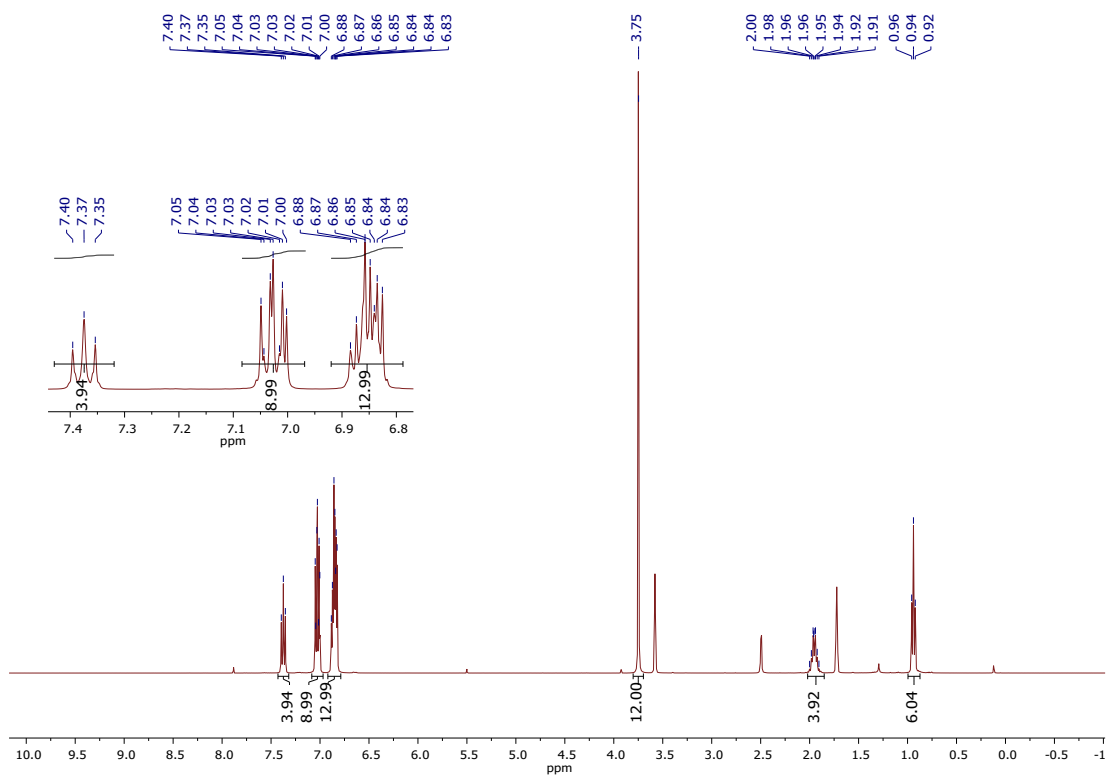


Fig. S26. ^1H NMR (400 MHz, THF-d_8 , 298 K) of compound **DTPA-Et**.

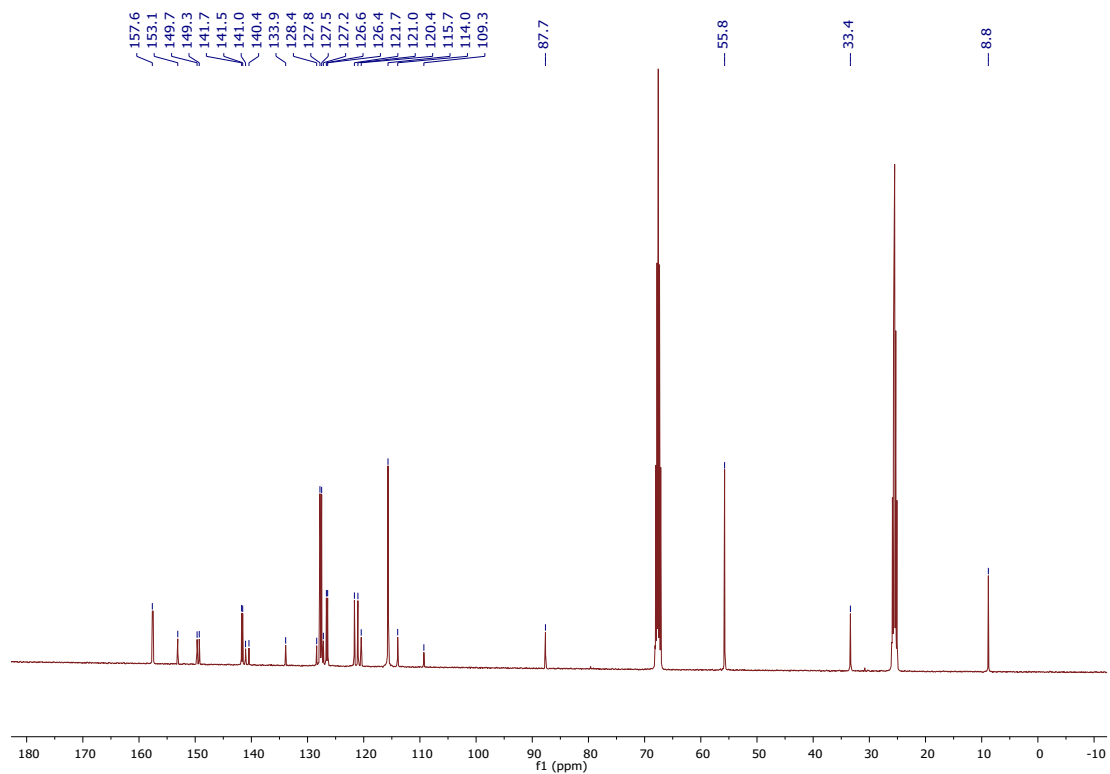


Fig. S27. ^{13}C NMR (100 MHz, THF- d_8 , 298 K) of compound DTPA-Et.

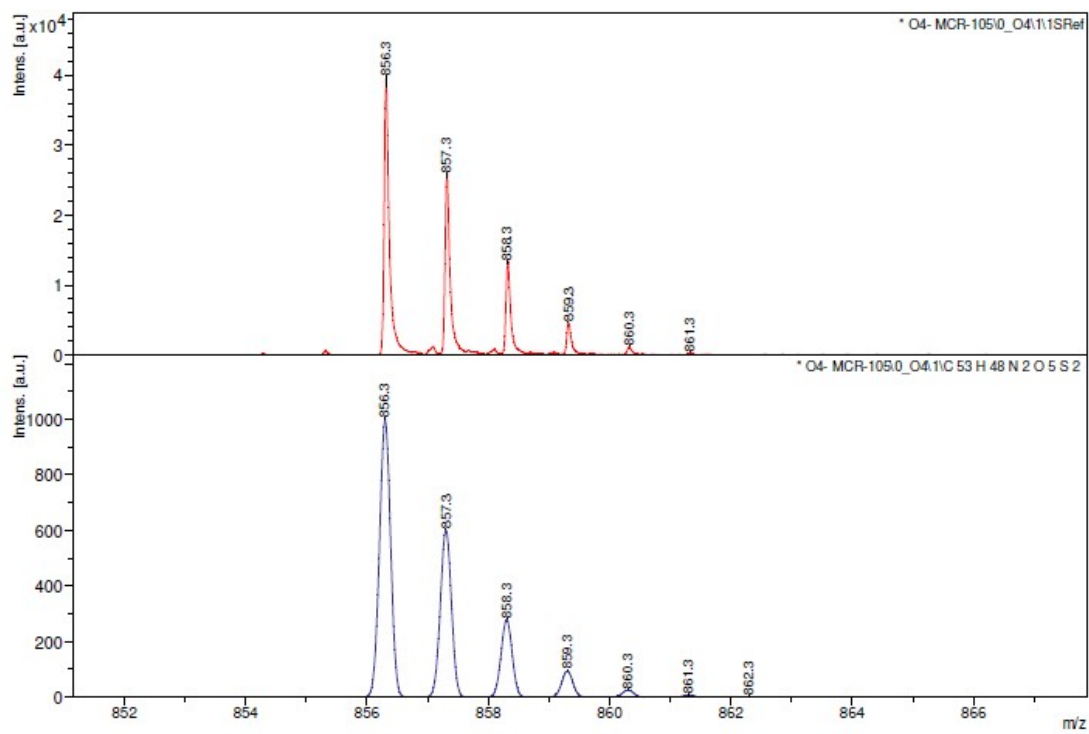


Fig. S28. HR-MALDI-TOF mass spectrum of compound DTPA-Et.

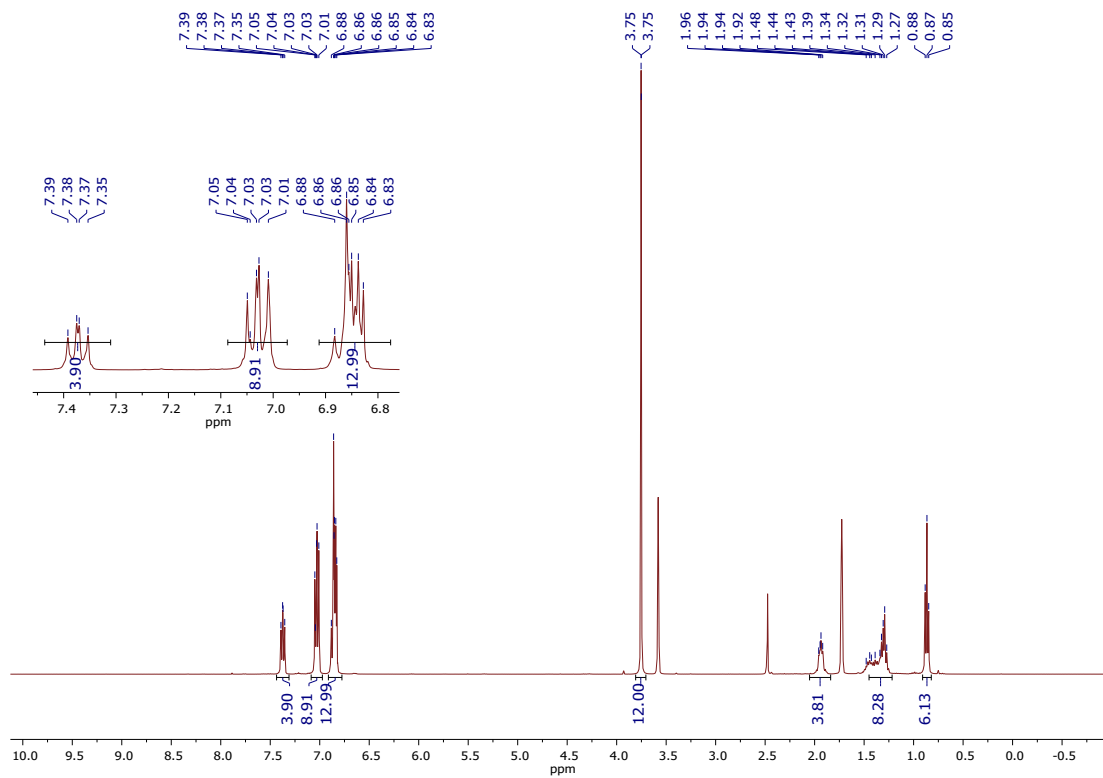


Fig. S29. ^1H NMR (400 MHz, $\text{THF-}d_8$, 298 K) of compound DTPA-Bu.

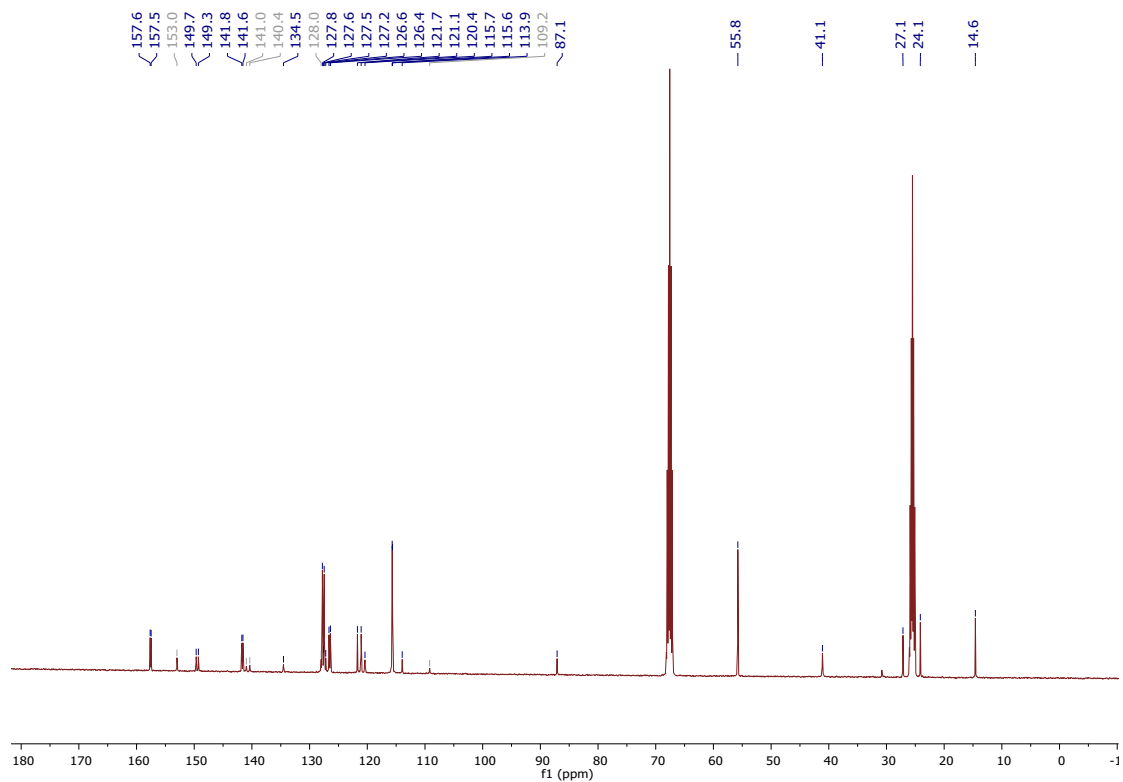


Fig. S30. ^{13}C NMR (100 MHz, $\text{THF-}d_8$, 298 K) of compound DTPA-Bu.

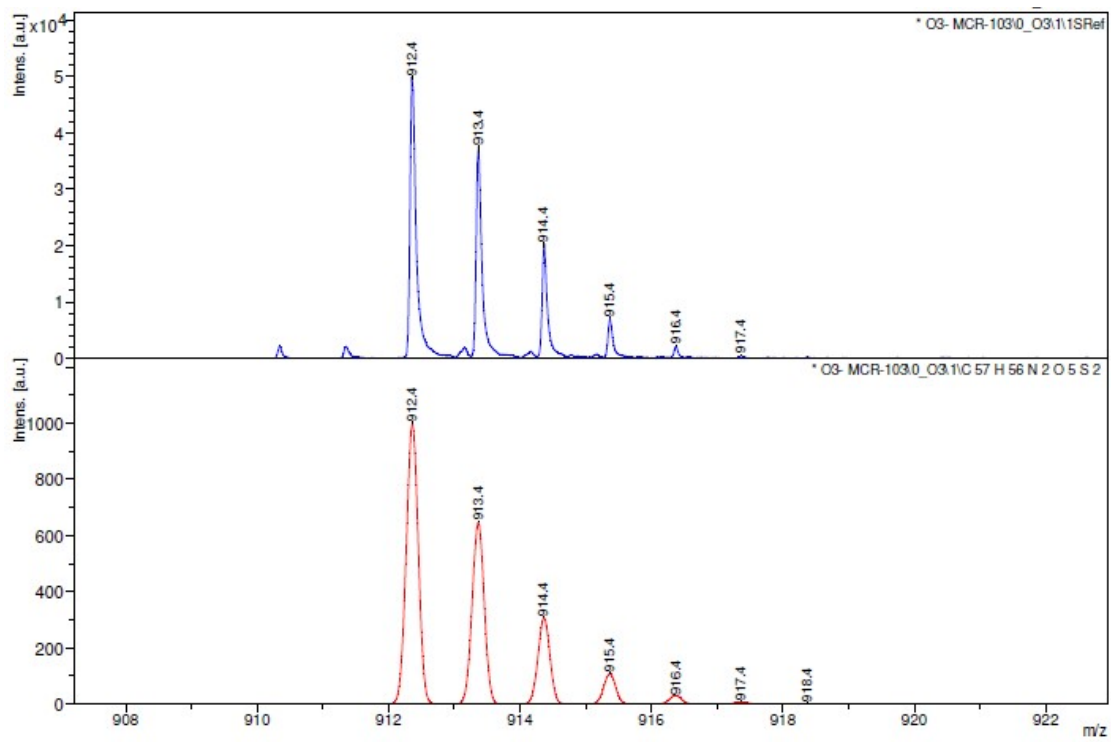


Fig. S31. HR-MALDI-TOF mass spectrum of compound DTPA-Bu.

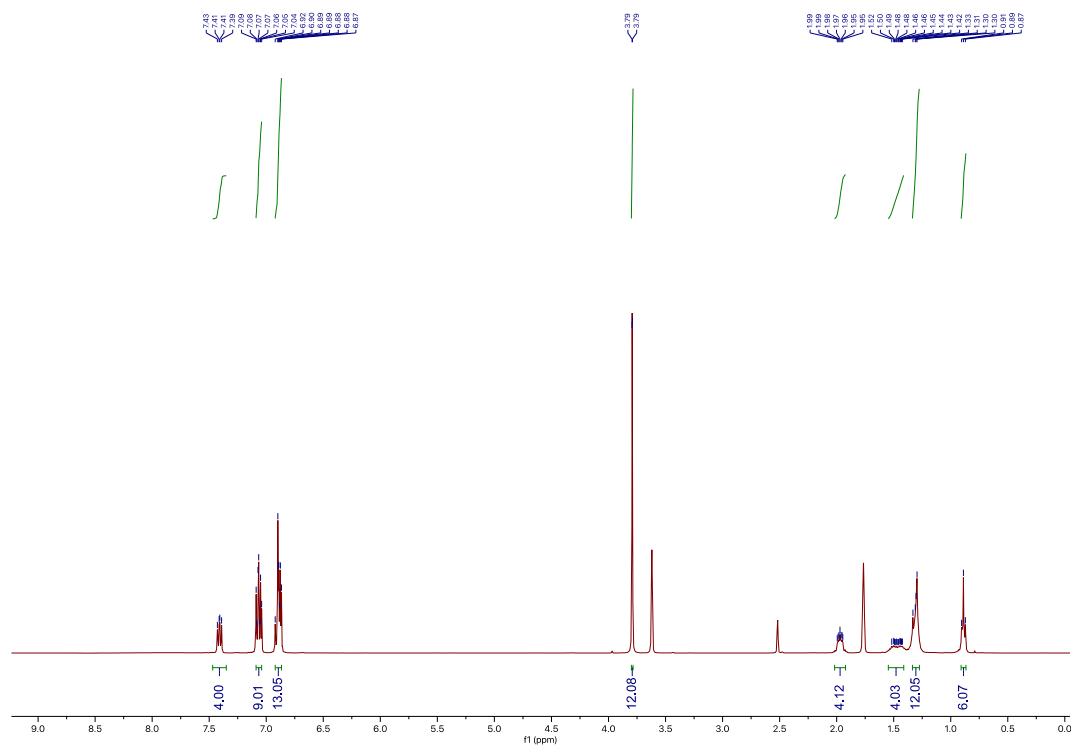


Fig. S32. ^1H NMR (400 MHz, THF-d_8 , 298 K) of compound DTPA-Hex.

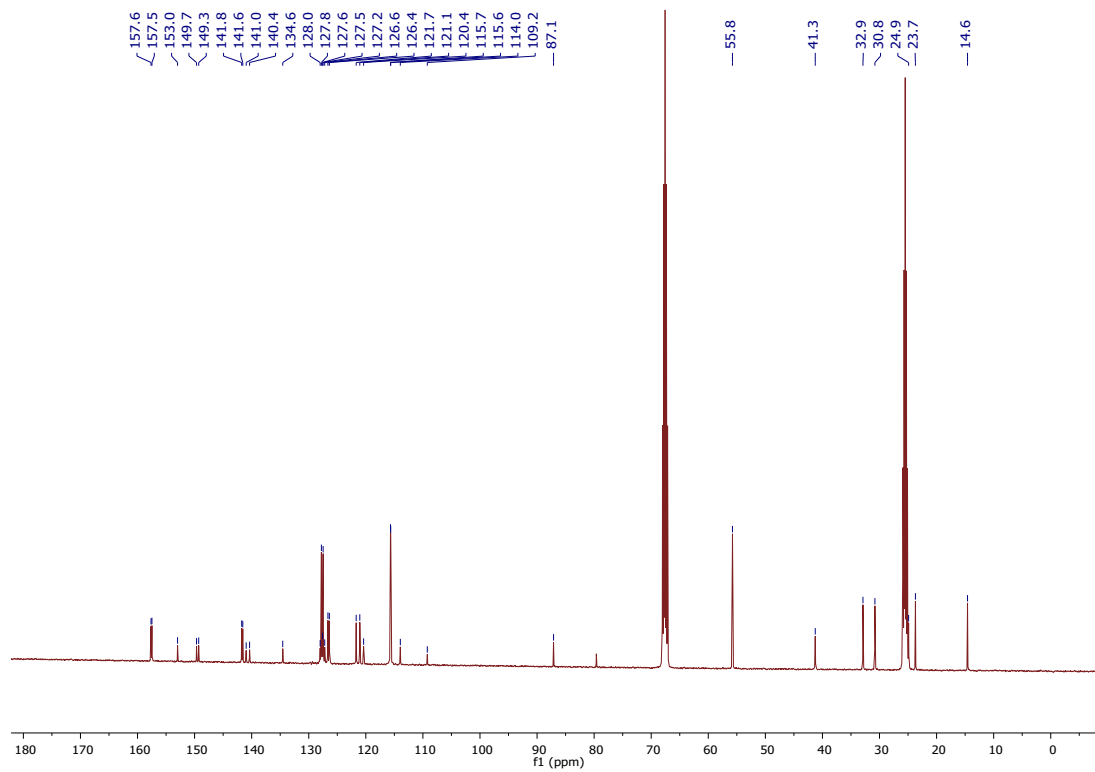


Fig. S33. ^{13}C NMR (100 MHz, $\text{THF-}d_8$, 298 K) of compound **DTPA-Hex**.

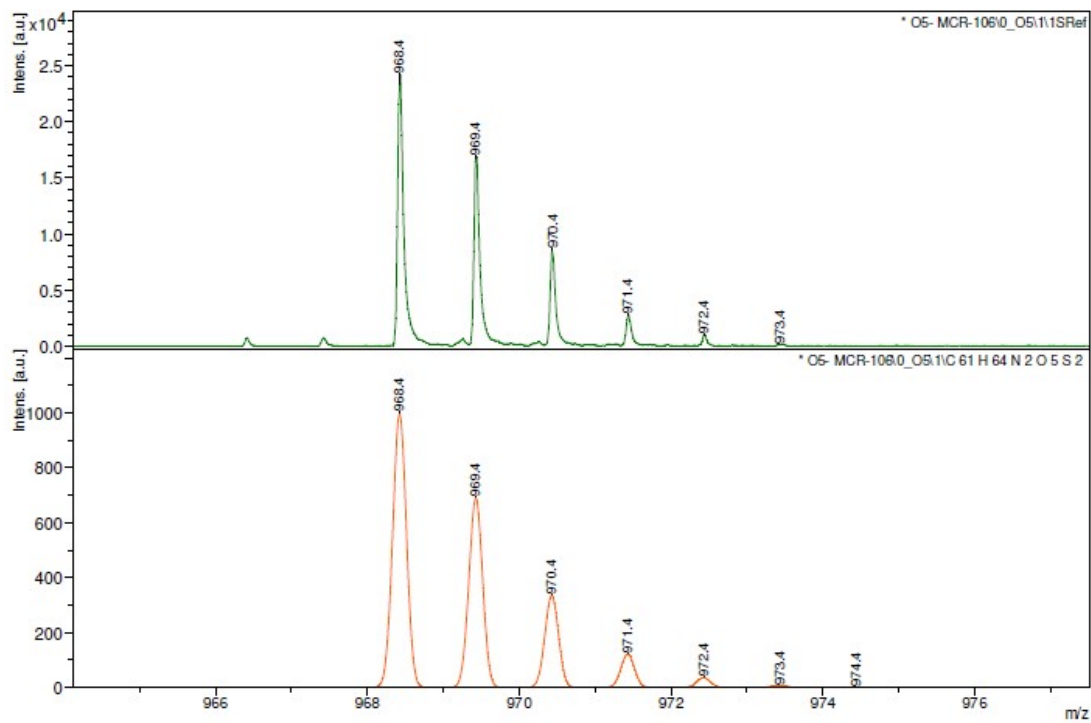


Fig. S34. HR-MALDI-TOF mass spectrum of compound **DTPA-Hex**.

References

- [1] J. Brebels, E. Douvogianni, D. Devisscher, R. Thiruvallur Eachambadi, J. Manca, L. Lutsen, D. Vanderzande, J. C. Hummelen, W. Maes, *J. Mater. Chem. C* **2018**, *6*, 500–511.
- [2] L. Dou, C. C. Chen, K. Yoshimura, K. Ohya, W. H. Chang, J. Gao, Y. Liu, E. Richard, Y. Yang, *Macromolecules* **2013**, *46*, 3384–3390.
- [3] C. Xia, H. Wu, Q. Yue, S. Chen, L. Shui, H. Fan, X. Zhu, *J. Mater. Chem. C* **2019**, *7*, 15344–15349.
- [4] A. D. Boese, J. M. L. Martin, *J. Chem. Phys.* **2004**, *121*, 3405–3416.
- [5] A. D. McLean, G. S. Chandler, *J. Chem. Phys.* **1980**, *72*, 5639–5648.
- [6] R. Krishnan, J. S. Binkley, R. Seeger, J. A. Pople, *J. Chem. Phys.* **1980**, *72*, 650–654.
- [7] A. V Marenich, R. M. Olson, C. P. Kelly, C. J. Cramer, D. G. Truhlar, *J. Chem. Theory Comput.* **2007**, *3*, 2011–2033.
- [8] A. V Marenich, C. J. Cramer, D. G. Truhlar, *J. Phys. Chem. B* **2009**, *113*, 6378–6396.
- [9] and D. J. F. M. J. Frisch, G. W. Trucks, H. B. Schlegel, G. E. Scuseria, M. A. Robb, J. R. Cheeseman, G. Scalmani, V. Barone, G. A. Petersson, H. Nakatsuji, X. Li, M. Caricato, A. V. Marenich, J. Bloino, B. G. Janesko, R. Gomperts, B. Mennucci, H. P. Hratchian, J. V. Ortiz, **2016**.
- [10] J. B. Maglic, R. Lavendomme, *J. Appl. Crystallogr.* **2022**, *55*, 1033–1044.
- [11] T. Lu, F. Chen, *J. Comput. Chem.* **2012**, *33*, 580–592.
- [12] C. A. Guido, P. Cortona, B. Mennucci, C. Adamo, *J. Chem. Theory Comput.* **2013**, *9*, 3118–3126.
- [13] J. Wang, H. Zhang, B. Wu, Z. Wang, Z. Sun, S. Xue, Y. Wu, A. Hagfeldt, M. Liang, *Angew. Chem. Int. Ed.* **2019**, *58*, 15721–15725.
- [14] J. A. Röhr, D. Moia, S. A. Haque, T. Kirchartz, J. Nelson, *J. Phys. Condens. Matter* **2018**, *30*, 105901.